Technical Review

No. 1 · 1989

STSF – a unique technique for scan-based Near-field Acoustic Holography without restrictions on coherence.

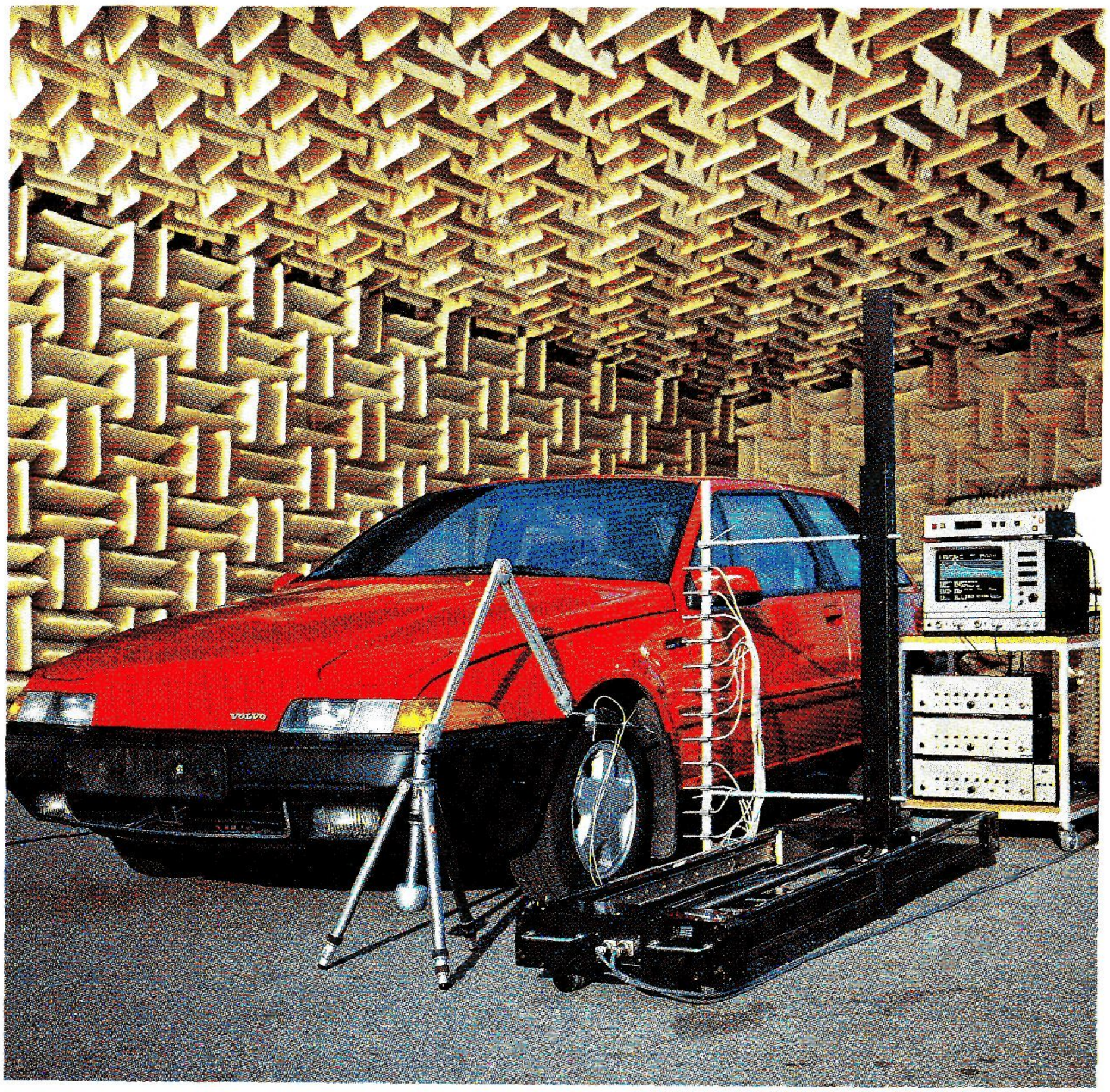

Brüel & Kjær

Previously issued numbers of Brüel & Kjær Technical Review

2–1988 Quantifying Draught Risk
1–1988 Using Experimental Modal Analysis to Simulate Structural Dynamic Modifications
Use of Operational Deflection Shapes for Noise Control of Discrete Tones
4–1987 Windows to FFT Analysis (Part II).
Acoustic Calibrator for Intensity Measurement Systems
3–1987 Windows to FFT Analysis (Part I)
2–1987 Recent Developments in Accelerometer Design
Trends in Accelerometer Calibration
1–1987 *Vibration Monitoring of Machines*
4–1986 Field Measurements of Sound Insulation with a Battery-Operated Intensity Analyzer
Pressure Microphones for Intensity Measurements with Significantly Improved Phase Properties
Measurement of Acoustical Distance between Intensity Probe Microphones
Wind and Turbulence Noise of Turbulence Screen, Nose Cone and Sound Intensity Probe with Wind Screen
3–1986 A Method of Determining the Modal Frequencies of Structures with Coupled Modes
Improvement to Monoreference Modal Data by Adding an Oblique Degree of Freedom for the Reference
2–1986 Quality in Spectral Match of Photometric Transducers
Guide to Lighting of Urban Areas
1–1986 Environmental Noise Measurements
4–1985 Validity of Intensity Measurements in Partially Diffuse Sound Field
Influence of Tripods and Microphone Clips on the Frequency Response of Microphones
3–1985 The Modulation Transfer Function in Room Acoustics
RASTI: A Tool for Evaluating Auditoria
2–1985 Heat Stress
A New Thermal Anemometer Probe for Indoor Air Velocity Measurements
1–1985 Local Thermal Discomfort
4–1984 Methods for the Calculation of Contrast
Proper Use of Weighting Functions for Impact Testing
Computer Data Acquisition from Brüel & Kjær Digital Frequency Analyzers 2131/2134 Using their Memory as a Buffer
3–1984 The Hilbert Transform
Microphone System for Extremely Low Sound Levels
Averaging Times of Level Recorder 2317
2–1984 Dual Channel FFT Analysis (Part II)
1–1984 Dual Channel FFT Analysis (Part I)
4–1983 Sound Level Meters – The Atlantic Divide
Design principles for Integrating Sound Level Meters

(Continued on cover page 3)

Technical Review

No. 1 · 1989

Contents

STSF – a unique technique for scan-based Near-field Acoustic Holography without restrictions on coherence

by Jørgen Hald

Abstract

The Spatial Transformation of Sound Fields (STSF) technique involves a scanning over a (planar) surface close to the source under investigation. From cross spectra measured during the scan, a principal component representation of the sound field is extracted. Any power descriptor of the near field (intensity, sound pressure, etc.) can then be investigated by means of Near-field Acoustic Holography (NAH), while the more distant field can be determined by application of Helmholtz' integral equation.

The present paper outlines the theoretical foundation of the cross spectral principal component technique implemented in STSF, and relates it to various other NAH techniques. It is demonstrated that compared to these techniques, the cross spectral formulation as implemented in STSF has the advantage that no restrictions are placed on the coherence and bandwidth of the sound field, without requiring simultaneous measurements.

Sommaire

La technique de transformation spatiale des champs sonores (Spatial Transformation of Sound Fields) est fondée sur le balayage d'une surface plane près de la source étudiée. Une représentation de la composante principale est extraite de l'interspectre mesuré pendant le balayage. Tout de-

scripteur de puissance du champ proche (intensité acoustique, pression acoustique, etc.) peut alors être étudié au moyen de l'holographie acoustique du champ proche (Near-field Acoustic Holography), alors que le champ plus distant peut être déterminé en appliquant l'équation intégrale de Helmholtz.

Cet article expose le fondement théorique de la technique de composante principale interspectrale employée en STSF, et la compare à d'autres techniques NAH. Il est démontré que comparée à ces techniques, la formulation interspectrale telle qu'employée en STSF a l'avantage de ne placer aucune rectriction sur les cohérence et largeur de bande du champ sonore, même si les mesures ne sont pas simultanées.

Zussammenfassung

Die räumlichen Transformation von Schallfeldern (STSF) beinhaltet das Abtasten einer (planen) Oberfläche nahe der zu untersuchenden Schallquelle. Aus den während des Abtastens gemessenen Kreuzspektren lassen sich zur Beschreibung des Schallfelds grundlegende Größen ableiten. Alle Leistungsgrößen des Nahfelds (Intensität, Schalldruck usw.) können mit Hilfe der Nahfeld-Holographie (NAH) untersucht werden; während das Fernfeld durch Anwendung der Helmholtz-Gleichung beschrieben wird.

Die vorliegende Arbeit beschreibt die theoretischen Grundlagen der in der STSF enthaltenen Kreuzspektren-Komponentenmethode und vergleicht sie mit verschiedenen anderen NAH-Methoden. Es wird herausgearbeitet, daß die Kreuzspektrenmethode im Unterschied zu den anderen Methoden den Vorteil hat, daß keine Beschränkungen bestehen bezüglich der Kohärenz und Bandbreite des Schallfelds und keine simultane Messungen erforderlich sind.

1. Introduction

1.1. Principle of STSF

The basic principle of the Spatial Transformation of Sound Fields (STSF) technique is illustrated in Fig. 1. Based on cross spectra measured over a planar surface close to the source under investigation, all parameters of the sound field can be mapped over a three dimensional region extending

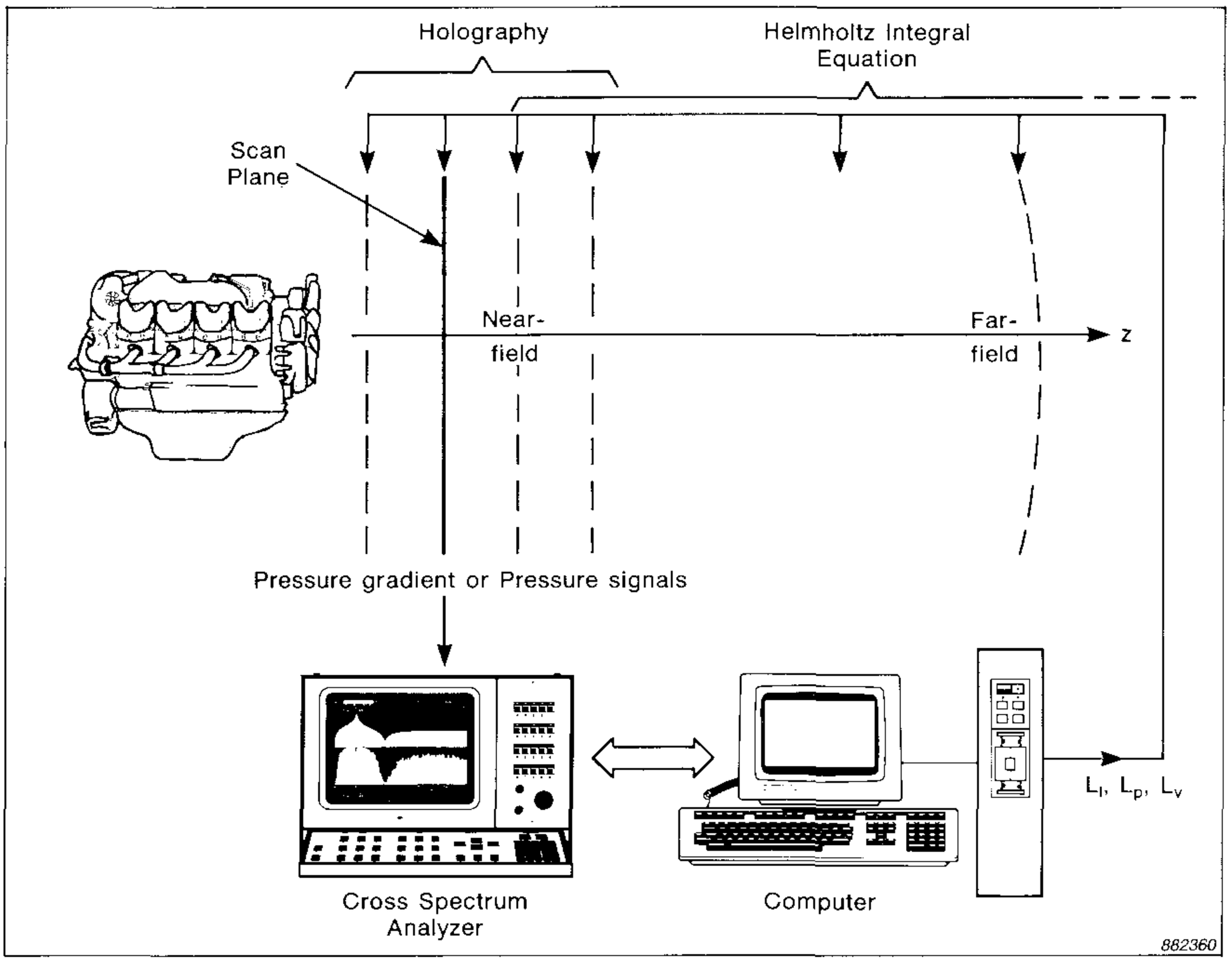

Fig. 1. Principle of STSF

from the surface of the source to infinity. The near field is predicted from the scan data using Near-field Acoustic Holography (NAH), while the more distant field is calculated using Helmholtz' Integral Equation (HIE).

In addition to the 3D mapping capability based on 2D measurements, STSF also provides the possibility of doing Partial Source Attenuation Simulation (PSAS). This simulation is done by backwards propagating the cross spectral representation of the sound field from the measurement surface to (ideally) the source surface, then modifying the representation at the source surface according to an attenuation model and finally predicting the sound field from the modified representation.

1.2. Development of STSF

Methods for prediction of a wave field in regions of space based on measurements in other regions have evolved over a long period. Most of the

techniques are based on Helmholtz' integral equation, which in principle requires, for the case of acoustic wave fields, the measurement of pressure and particle velocity over a surface enclosing the source. Some aspects of the recent development shall be outlined.

Parrent [1] derived an alternative formulation of Helmholtz' integral equation to propagate mathematically the mutual coherence function from a source surface to sets of points further away from the source. Thus, a statistical description of the wave fields had been interconnected with the mathematical propagation models, allowing better modelling of the propagation of non-coherent fields.

The theory developed by Parrent and other scientists in the field of optics led to similar work within the field of acoustics. Ferris [2] showed how the far-field sound pressure could be predicted from the cross spectra measured over a surface enclosing the source in the near-field region.

The work of Shewell and Wolf [3] on inverse diffraction of monochromatic (single frequency) coherent wave fields constitutes a basis for acoustic holography. Their plane to plane diffraction theory allows prediction of the field closer to the source than the measurement plane. Evanescent waves are, however, not reconstructed which is usually not serious in optics but of great importance in acoustics, where the wavelength is often not small compared to the size of the source.

This fundamental drawback of the inverse diffraction technique was removed in the Near-field Acoustic Holography technique introduced by Williams, Maynard and Skudrzyk from Pennsylvania State University [4]. In NAH the evanescent waves are reconstructed to an extent which is limited basically by the dynamic range of the measured data.

Since the first presentation of NAH, the technique has been improved, and the underlying theory has been explored and published in a number of papers, recently in a review paper by Maynard, Williams and Lee [5]. This paper also describes a couple of complete NAH systems built at Pennsylvania State University.

The STSF system developed at Brüel & Kjær, Denmark, applies NAH and HIE in connection with a cross spectral description of the sound field [6 – 11]. By doing so, the coherence and single frequency restrictions in conventional implementations of NAH and HIE are avoided, as will be demonstated in the present paper. The STSF system includes an efficient principal component measurement technique to achieve a cross spectral representation of the sound field.

2. Spatial transformation tools for complex time harmonic sound fields

Throughout this paper the word monochromatic will be used to describe a wave field which has only a single frequency component. Similarly, a coherent wave field is a field with perfect coherence between every pair of points.

The mathematical models for the propagation of sound waves in a homogeneous source free medium are based on the homogeneous wave equation. For a single frequency component with angular frequency ω and wave number $k = \omega/c$, c being the propagation velocity of sound in the medium, the wave equation takes the form [12]

$$\nabla^2 p(\underline{r}) + k^2 p(\underline{r}) = 0 \tag{1}$$

Here ∇^2 is the Laplace operator which can also be expressed as the divergence of the gradient ($\nabla^2 = \underline{\nabla} \cdot \underline{\nabla}$), p is the complex sound pressure with an assumed time dependence $e^{j\omega t}$, and $\underline{r}$ describes the position in space.

In connection with the wave equation (1) it is important to realize that it has been obtained by a Fourier transform of the corresponding temporal wave equation. The complex wave field $p(\underline{r}, \omega)$ in eq. (1) should therefore be seen as the Fourier transform of a single, infinite, time record of a field $p(\underline{r}, t)$. This fact must be borne in mind when measurements are taken in a wave field to be processed using the wave equation (1). Either the data must be taken simultaneously, or some kind of periodicity or repeatability of the time signal must be exploited.

In any case, the time harmonic field represented by $p(\underline{r}, \omega)$ is monochromatic and perfectly coherent. A coherence less than one cannot be represented by a single time harmonic field. From the application of dual channel FFT analyzers it is commonly known that a single set of Fourier transformed, simultaneous time records cannot represent a coherence less than one. As the wave equation (1) is based on a single Fourier transformed time record, it cannot predict a coherence less than one. The prediction of statistical descriptors such as coherence requires several independent Fourier transformed time records.

2.1. Helmholtz' Integral Equation (HIE)

The Helmholtz' integral equation can be derived on the basis of the homogeneous wave equation (1), see e.g. [12]. In its general form HIE expresses

the wave field $p(\underline{r})$ at a position $\underline{r}$ outside a closed surface S enclosing the source in terms of the wave field itself and its normal derivative on the surface S:

$$p(\underline{r}) = \int_S \left\{ \frac{\partial p(\underline{r}')}{\partial n} G(\underline{r}, \underline{r}') - p(\underline{r}') \frac{\partial G(\underline{r}, \underline{r}')}{\partial n} \right\} dS(\underline{r}') \tag{2}$$

In this equation $\partial/\partial n$ means differentiation in the direction of the outwards unit normal to the surface S, $\underline{r}'$ defines a position on S, $dS(\underline{r}')$ is a surface area element at $\underline{r}'$, and G is the free space Green's function,

$$G(\underline{r}, \underline{r}') = \frac{e^{-jk|\underline{r}-\underline{r}'|}}{4\pi|\underline{r}-\underline{r}'|} \tag{3}$$

The normal derivative of the sound pressure in eq. (2) can be replaced by the normal component u_n of the particle velocity through application of the equation of motion [13]

$$\frac{\partial p}{\partial n} = -j\omega\rho u_n \tag{4}$$

where ρ is the density of the medium. Substitution of eq. (4) in eq. (2) now leads to the following general form of HIE

$$p(\underline{r}) = -\int_S \left\{ j\omega\rho u_n(\underline{r}') G(\underline{r}, \underline{r}') + p(\underline{r}') \frac{\partial G(\underline{r}, \underline{r}')}{\partial n} \right\} dS(\underline{r}') \tag{5}$$

Fig. 2 illustrates the geometry referred to in eq. (5).

Noting that the surface S can be any surface enclosing the source, we select as S a plane close to the source, closed by a hemisphere at infinity, ref. Fig. 2b. With this choice of S, the Sommerfeld radiation condition can be used to show that only the plane contributes to the integral in eq. (5), [12].

Further, instead of the free space Green's function $G(\underline{r}, \underline{r}')$, we may select a Green's function $G_p(\underline{r}, \underline{r}')$ that vanishes on the planar surface S, see e.g. [12]. Using this Green's function, the general form (5) of HIE simplifies to

$$p(\underline{r}) = -\int_S p(\underline{r}') \frac{\partial G_p(\underline{r}, \underline{r}')}{\partial n} dS(\underline{r}') \tag{6}$$

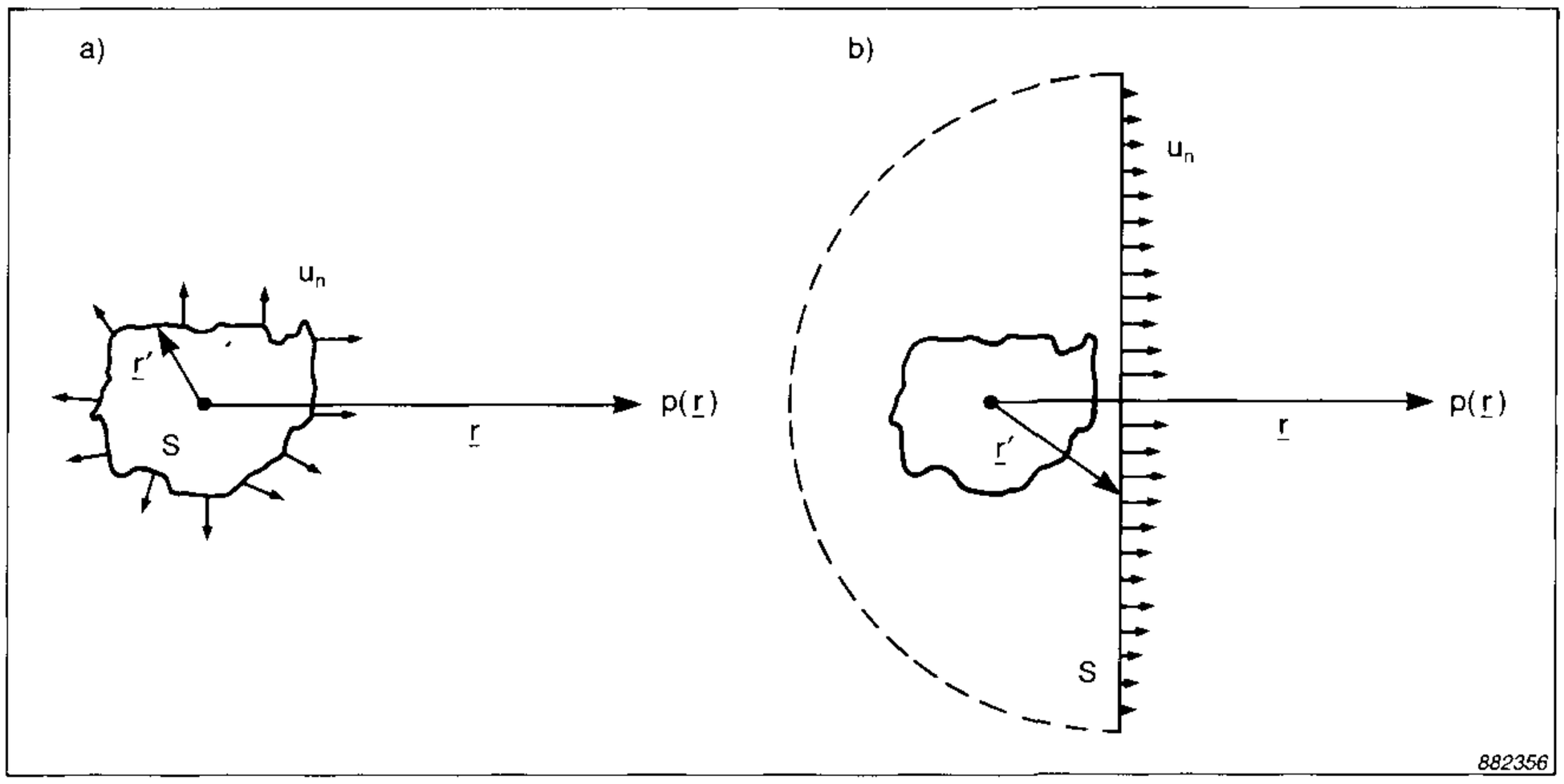

Fig. 2. Geometry used in Holmholtz' Integral Equation (HIE)
a) Complicated measurement surface S
b) Planar measurement surface S

which requires only the pressure field to be known on S. Reference [12] gives an expression for $G_p(\underline{r}, \underline{r}')$ allowing eq. (6) to be rewritten in the following form

$$p(\underline{r}) = j\int_S p(\underline{r}')\cos\theta\left(1-\frac{j}{kR}\right)\frac{e^{-jkR}}{\lambda R}\,dS(\underline{r}') \tag{7}$$

where λ is wavelength, $\underline{R} \equiv \underline{r} - \underline{r}'$ is the vector from the integration point $\underline{r}'$ on the surface S to the field point $\underline{r}$, $R \equiv |\underline{R}|$ is the length of this vector, and θ is the angle from the outward surface normal $\hat{n}$ (at $\underline{r}'$) to $\underline{R}$, that is: $\cos\theta = \hat{n} \cdot \underline{R}/R$.

Instead of $G_p(\underline{r}, \underline{r}')$ we might have selected a Green's function $G_u(\underline{r}, \underline{r}')$ with vanishing normal derivative over the measurement surface S. This would lead to a formulation requiring only the normal component u_n of the particle velocity to be known over S. These two special formulations of HIE are historically referred to as the first and second Rayleigh integrals respectively [5].

For practical applications of e.g. Rayleigh's first integral (7), measurements are taken only at a discrete set of points, $\underline{r}'_n$, $n = 1, 2, ..., N$, over a finite measurement area, and the integral is approximated by a summation

$$p(\underline{r}) \approx \sum_{n=1}^{N} p(\underline{r}'_n)\ H(\underline{r}, \underline{r}'_n) \tag{8}$$

with

$$H(\underline{r}, \underline{r}'_n) = j\cos\theta_n \left(1 - \frac{j}{kR_n}\right) \frac{e^{-jkR_n}}{\lambda R_n} \Delta S_n \tag{9}$$

where in general the subscript "n" refers to measurement point no. n at $\underline{r}'_n$, and ΔS_n is the surface area element at that point.

Arranging the measured pressure data $p(\underline{r}'_n)$ in a column matrix $\boldsymbol{p}$,

$$\boldsymbol{p} \equiv \begin{bmatrix} p(\underline{r}'_1) \\ p(\underline{r}'_2) \\ \vdots \\ p(\underline{r}'_N) \end{bmatrix} \tag{10}$$

and similarly the transfer functions $H(\underline{r}, \underline{r}'_n)$ in another column matrix $\boldsymbol{H}(\underline{r})$,

$$\boldsymbol{H}(\underline{r}) \equiv \begin{bmatrix} H(\underline{r}, \underline{r}'_1) \\ H(\underline{r}, \underline{r}'_2) \\ \vdots \\ H(\underline{r}, \underline{r}'_N) \end{bmatrix} \tag{11}$$

allows the Rayleigh formula (8) to be written in the following condensed matrix form:

$$p(\underline{r}) \approx \boldsymbol{H}^T(\underline{r})\, \boldsymbol{p} = \boldsymbol{p}^T\, \boldsymbol{H}(\underline{r}) \tag{12}$$

2.2. Near-field Acoustic Holography (NAH)

A detailed description of the theory behind NAH has been given in the literature, [4–5], and reference [14] treats some important aspects of computer implementations of the NAH algorithms.

The treatment to be given here will be a high-level matrix oriented description based on the formulation of HIE in the foregoing section. In the context of the present paper, NAH is considered a tool that applies for

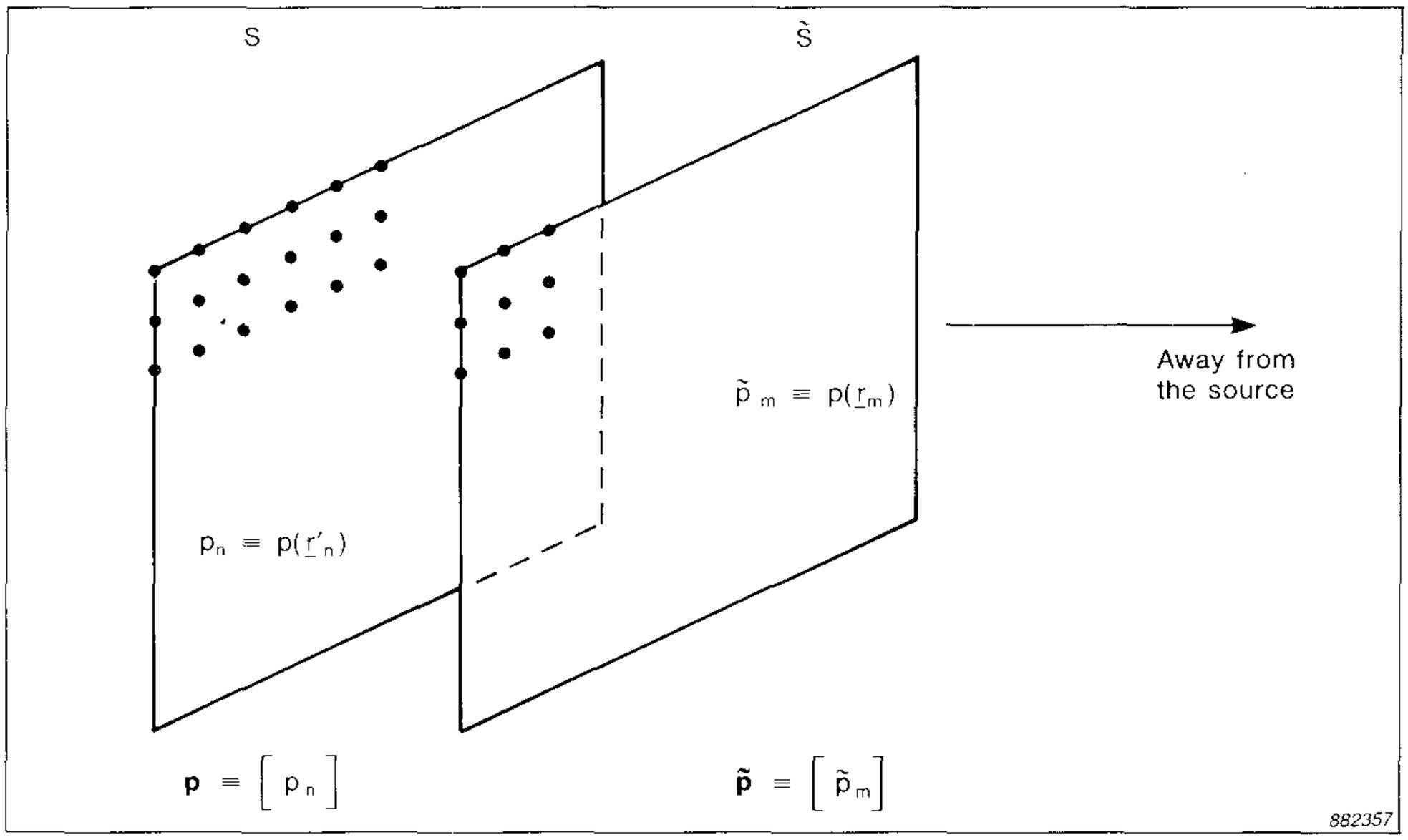

Fig. 3. Hologram plane S and calculation plane $\tilde{S}$ with hologram matrix $\boldsymbol{p}$ and output matrix $\tilde{\boldsymbol{p}}$ respectively

plane to plane transformation of complex time harmonic sound fields, taking into account the evanescent wave components of the near field.

More specifically the problem solved by NAH is the following. Having measured the complex (time harmonic) pressure $p(\underline{r}')$ over a plane S close to the source, the pressure $p(\underline{r})$ over a translated plane $\tilde{S}$ is calculated. Since the measured pressure function $p(\underline{r}')$ shall be denoted the hologram, the measurement plane S will be referred to as the hologram plane. The calculation plane $\tilde{S}$ can be either further away from or closer to the source than the hologram plane, see Fig. 3, the only requirement being that the region between S and $\tilde{S}$ is source free.

As in the previous section we define a grid of measurement points $\underline{r}'_n$ in the hologram plane, and arrange the complex pressures $p_n \equiv p(\underline{r}_n)$ measured at these points in a column matrix $\boldsymbol{p}$. This matrix which shall be denoted the hologram matrix was defined in eq. (10).

Instead of the single output point $\underline{r}$ defined in connection with HIE, we now define a complete grid of output points $\underline{r}_m$, $m = 1, 2, \ldots M$, on the calculation plane $\tilde{S}$. We will assume that the hologram and output grids are equal, and thus $M = N$.

To be able to use the HIE formula (12) for calculation of the pressure $\tilde{p}_m \equiv p(\underline{r}_m)$ at $\underline{r}_m$, we assume first that $\tilde{S}$ is further away from the source

than S. Defining the column matrix $\boldsymbol{H}_m$ of Green's function values to the point $\underline{r}_m$ as

$$\boldsymbol{H}_m \equiv \boldsymbol{H}(\underline{r}_m) \tag{13}$$

where $\boldsymbol{H}(\underline{r}_m)$ is defined in eq. (11), then according to eq. (12) $\tilde{p}_m$ is given by

$$\tilde{p}_m = \boldsymbol{H}_m{}^T \boldsymbol{p} = \boldsymbol{p}^T \boldsymbol{H}_m \tag{14}$$

Here, the superscript "T" specifies a transposition of a matrix.

As a final step to achieve a matrix description of the plane to plane transform, we define a column matrix $\tilde{\boldsymbol{p}}$ containing the estimated pressures $\tilde{p}_m$

$$\tilde{\boldsymbol{p}} \equiv \begin{bmatrix} \tilde{p}_1 \\ \tilde{p}_2 \\ \vdots \\ \tilde{p}_M \end{bmatrix} \tag{15}$$

and a matrix $\boldsymbol{H}$ consisting of the Green's function column matrices $\boldsymbol{H}_m$

$$\boldsymbol{H} \equiv \begin{bmatrix} \boldsymbol{H}_1{}^T \\ \boldsymbol{H}_2{}^T \\ \vdots \\ \boldsymbol{H}_M{}^T \end{bmatrix} \tag{16}$$

Then from eqs. (14), (15) and (16) we obtain

$$\tilde{\boldsymbol{p}} = \boldsymbol{H}\ \boldsymbol{p} \tag{17}$$

expressing the transform from S to $\tilde{S}$ as a linear transform of the hologram matrix $\boldsymbol{p}$.

In the derivation of the transform formula (17), no advantage was taken of symmetries or of the fact that the transform from S to S has the form of a two-dimensional spatial convolution. The convolution property is inherent in the Rayleigh integral (7) since both R and θ depend on $\underline{r}$ and $\underline{r}'$ only through $\underline{r} - \underline{r}'$.

Due to its convolution property, the linear transform (17) from S to $\tilde{S}$ can be done much more effectively through the use of two-dimensional

spatial Fourier transforms instead of the direct discrete integration of the Rayleigh integral, [12]. In the two-dimensional spatial frequency domain the convolution is performed by multiplication of the individual spatial frequencies with a complex transfer function. Since both Fourier transforms and multiplication with a transfer function are linear transformations, they can be visualized as multiplications with transform matrices. In other words, if by the matrix $\boldsymbol{F}$ we represent a spatial two-dimensional Discrete Fourier Transform (DFT), and by the diagonal matrix $\boldsymbol{T}$ a transfer function multiplication, then $\boldsymbol{F}^{-1}$ represents the inverse spatial two-dimensional DFT and therefore the transform from S to $\tilde{S}$ can be written as

$$\tilde{\boldsymbol{p}} = \boldsymbol{F}^{-1}\ \boldsymbol{T}\ \boldsymbol{F}\ \boldsymbol{p} \tag{18}$$

Note that the matrices $\boldsymbol{F}$, $\boldsymbol{T}$ and $\boldsymbol{F}^{-1}$ are never actually calculated. They just represent the corresponding linear transforms.

Now, if instead of eq. (16) we use the following definition of the transform matrix $\boldsymbol{H}$,

$$\boldsymbol{H} \equiv \boldsymbol{F}^{-1}\ \boldsymbol{T}\ \boldsymbol{F} \tag{19}$$

then the transform from S to $\tilde{S}$ can still be expressed as in eq. (17),

$$\tilde{\boldsymbol{p}} = \boldsymbol{H}\ \ \boldsymbol{p} \tag{20}$$

However, in eq. (20) $\boldsymbol{H}$ is used only to represent the linear transforms $\boldsymbol{F}$, $\boldsymbol{T}$ and $\boldsymbol{F}^{-1}$ comprising the NAH transform tool.

In the formulation (19) of the plane to plane transform, the diagonal matrix $\boldsymbol{T}$ expresses the translation, and thus it depends on the translation distance z away from the source,

$$\boldsymbol{T} = \boldsymbol{T}(z) \tag{21}$$

Since a translation z , $z > 0$, followed by the opposite translation $-z$, must leave the original data unchanged, the following relation must hold:

$$\boldsymbol{T}(-z) = \boldsymbol{T}^{-1}(z) \tag{22}$$

which defines the transform matrix $\boldsymbol{H} = \boldsymbol{F}^{-1}\boldsymbol{T}(-z)\,\boldsymbol{F}$ for a translation $-z$ towards the source. In this process the amplification of evanescent waves is represented by large values on the diagonal of $\boldsymbol{T}(-z)$.

As described in references [5] and [14], the calculation of a component (e.g. the normal component) of the particle velocity can be done by means of another transfer function $\boldsymbol{T}_u(z)$ instead of $\boldsymbol{T}(z)$, leading to another

transform matrix $\boldsymbol{H}_u$. In other words, the column matrix $\tilde{\boldsymbol{u}}$ of particle velocity data in the calculation plane can be expressed in the form

$$\tilde{\boldsymbol{u}} = \boldsymbol{H}_u \, \boldsymbol{p} \tag{23}$$

with

$$\boldsymbol{H}_u \equiv \boldsymbol{F}^{-1} \, \boldsymbol{T}_u(z) \, \boldsymbol{F} \tag{24}$$

In conclusion, the present section has given a matrix formulation of the transforms used in NAH. For details of the transformations and for a discussion of problems such as spatial aliasing, wrap-around errors and measurement bandwidth, the reader is referred to the references. The matrix formulation will be useful for the description of how NAH can be applied in connection with a cross spectral representation of the sound field.

Note, that the HIE and NAH transform formulae (17) and (20) have the same form, the difference being the content and practical implementation of the transform matrix $\boldsymbol{H}$.

3. The cross spectral approach to spatial transformation

As stated in connection with the wave equation (1), the direct use of this equation through e.g. HIE or NAH puts some restrictions on the technique applied for acquisition of input data. In connection with a general stationary random sound source, only simultaneous measurements at all input data points meet the requirements. Further, spatial transformation of a single Fourier transformed time record of the field achieved this way through simultaneous recording cannot predict statistical properties of the wave field associated with a coherence less than one.

All these limitations can be overcome by switching to a cross spectral description of the sound field. The cross spectrum function over the hologram plane will prove to constitute a complete representation of the sound field in the sense that it allows prediction of any of the power descriptors of the field over a three dimensional region extending from the source surface to infinity. Any degree of coherence can be handled by the cross spectral description. Broad-band sources can be handled by measurement in a set of limited frequency bands.

Two major problems shall be treated: How do we with a minimum of data acquisition obtain a full representation of the cross spectrum function over the hologram area, and how do we apply the NAH and HIE transforma-

tions in connection with the cross spectral representation of the sound field.

In the first and major part of this chapter we shall assume a monochromatic, non-coherent sound field. The implications of a finite frequency bandwidth are discussed in section 3.3.8.

3.1. The cross spectral sound field representation

To introduce the cross spectral representation of a sound field, assume first a time harmonic sound field with complex pressure function $p(\underline{r}')$ over the hologram plane S and complex hologram matrix $\boldsymbol{p} = [p_n]$ of pressures at the grid of measurement points $\underline{r}'_n$, see Fig. 3.

Assuming power normalization of the complex pressure function $p(\underline{r}')$, the cross-power spectrum $C_{n\nu}$ between grid points n and ν can be expressed as

$$C_{n\nu} = p_n^{\star} p_\nu \tag{25}$$

which leads to the following expression for the cross-power spectrum matrix $\boldsymbol{C}$ containing the cross spectra between every pair (n, ν) of measurement positions:

$$\boldsymbol{C} = \boldsymbol{p}^{\star} \boldsymbol{p}^{T} = \begin{bmatrix} p_1^{\star} \\ p_2^{\star} \\ \vdots \\ p_N^{\star} \end{bmatrix} \begin{bmatrix} p_1 \, p_2 \, \dots \, p_N \end{bmatrix} \tag{26}$$

This matrix $\boldsymbol{C}$ shall also be denoted the cross spectrum hologram matrix. In the formulae above, the superscript "$\star$" specifies a complex conjugation.

Similarly, the cross spectrum $\tilde{C}_{m\mu}$ between grid points $\underline{r}_m$ and $\underline{r}_\mu$ on the calculation plane $\tilde{S}$ can be expressed as

$$\tilde{C}_{m\mu} = \tilde{p}_m^{\star} \tilde{p}_\mu \tag{27}$$

and the expression for the cross spectrum matrix $\tilde{\boldsymbol{C}}$ containing the cross spectra between every pair (m, μ) of output points becomes

$$\tilde{\boldsymbol{C}} = \tilde{\boldsymbol{p}}^{\star} \tilde{\boldsymbol{p}}^{T} \tag{28}$$

Thus, for the case of a complex time harmonic sound field, the cross spectrum matrices $\boldsymbol{C}$ and $\tilde{\boldsymbol{C}}$ can be completely reconstructed from the complex pressure column matrices $\boldsymbol{p}$ and $\tilde{\boldsymbol{p}}$ respectively.

Consider next the general case of a non-coherent sound field. We need a mathematical model for such a sound field and its cross spectrum matrices $\boldsymbol{C}$ and $\tilde{\boldsymbol{C}}$ that allow application of the previously described spatial transformation tools for complex time harmonic fields.

For this, assume that the field is created by a set of L mutually uncorrelated partial sources, each radiating a corresponding partial field. Assuming each one of the partial sources to be a stationary random source and the corresponding partial field to be perfectly coherent (in the relevant regions) means that the coherence and cross spectra for that partial field can be obtained from the Fourier transform of a single, infinite, time record of the field. We shall therefore represent each of the partial fields by such a single Fourier transformed time record. Thus, for each frequency ω the single partial field is complex time harmonic, allowing the previously defined transform tools to be applied.

Denote by $\boldsymbol{p}_l$ the complex hologram matrix for partial source no. l, $l = 1, 2, \ldots, L$. Then according to eq. (26) the cross spectrum hologram matrix $\boldsymbol{C}_l$ for partial source no. l alone takes the form

$$\boldsymbol{C}_l = \boldsymbol{p}_l^{\star} \boldsymbol{p}_l^{T} \tag{29}$$

The cross spectrum hologram matrix $\boldsymbol{C}$ for the total sound field can now be obtained by observing the fact that the partial sources are mutually uncorrelated. Because of this fact, the corresponding radiated partial fields $p_l(\underline{r})$ are also mutually uncorrelated, implying that they contribute independently to cross-power spectra measured in the sound field:

$$\boldsymbol{C} = \sum_{l=1}^{L} \boldsymbol{C}_l \tag{30}$$

Similarly, in the output plane $\tilde{S}$ the total cross spectrum matrix $\tilde{\boldsymbol{C}}$ equals the sum of the cross spectrum matrices $\tilde{\boldsymbol{C}}_l$ from the partial sources

$$\tilde{\boldsymbol{C}} = \sum_{l=1}^{L} \tilde{\boldsymbol{C}}_l \tag{31}$$

where $\tilde{\boldsymbol{C}}_l$ can be expressed as

$$\tilde{\boldsymbol{C}}_l = \tilde{\boldsymbol{p}}_l^{\star} \tilde{\boldsymbol{p}}_l^{T} \tag{32}$$

$\tilde{\boldsymbol{p}}_1$ being the complex pressure column matrix for partial source no. l in the output plane $\tilde{S}$.

A convenient compact matrix representation of the sum formulae (30) and (31) can be achieved by introducing matrices $\boldsymbol{P}$ and $\tilde{\boldsymbol{P}}$ the columns of

which are the complex pressure column matrices $\boldsymbol{p}_l$ and $\tilde{\boldsymbol{p}}_l$ respectively, for the uncorrelated partial sources:

$$\boldsymbol{P} \equiv \left[\boldsymbol{p}_1 \ \boldsymbol{p}_2 \ \cdots \ \boldsymbol{p}_L \right] \tag{33}$$

$$\tilde{\boldsymbol{P}} \equiv \left[\tilde{\boldsymbol{p}}_1 \ \tilde{\boldsymbol{p}}_2 \ \cdots \ \tilde{\boldsymbol{p}}_L \right] \tag{34}$$

Use of these matrices allows the sum formulae to be rewritten in the following way:

$$\boldsymbol{C} = \boldsymbol{P}^{\star}\boldsymbol{P}^{T} \tag{35}$$

$$\tilde{\boldsymbol{C}} = \tilde{\boldsymbol{P}}^{\star}\tilde{\boldsymbol{P}}^{T} \tag{36}$$

A couple of concepts which will be useful in a subsequent analysis of the STSF technique shall be introduced. The hologram column matrix $\boldsymbol{p}_l$ for each one of the uncorrelated partial fields will also be denoted as the trace of that partial field over the hologram grid. Thus, each column of $\boldsymbol{P}$ represents the trace of a corresponding partial field over the hologram grid. Considering any one of the rows of $\boldsymbol{P}$ it contains the complex signal from the L partial fields measured at a single hologram grid position. Each row of $\boldsymbol{P}$ shall therefore be denoted as the view of the L partial fields as seen from the particular hologram grid position. Two points have independent views, if the L partial fields are seen with different mutual complex ratios at the two points.

Notice that a view of the partial fields assigns implicitly mutual phases to the uncorrelated partial fields. These mutual phases are arbitrary, being determined by the arbitrary selection of the time record defining the partial holograms $\boldsymbol{p}_l$, and therefore they should not be given any physical interpretation. This will be discussed later.

In connection with the expressions (35) and (36) for the cross spectrum matrices $\boldsymbol{C}$ and $\tilde{\boldsymbol{C}}$, it is important to realize that usually the number of independent sources L is much smaller than the number of measurement positions N in the hologram plane:

$$L \ll N \tag{37}$$

Therefore, if the individual independent sources could be identified and the corresponding partial holograms $\boldsymbol{p}_l$ be measured, then a representation of the cross spectrum hologram matrix $\boldsymbol{C}$ in terms of the matrix $\boldsymbol{P}$ of partial holograms might be very advantageous. The matrix $\boldsymbol{C}$ is of dimension $N \times N$ while $\boldsymbol{P}$ has only L columns and N rows. But in general we cannot identify the true independent partial sources.

However, equation (35) also provides us with the more general information that the rank of $\boldsymbol{C}$ cannot exceed the number L of independent partial sources. In mathematical terms, denoting by I the rank of $\boldsymbol{C}$:

$$I \equiv \text{rank}\,(\boldsymbol{C}) \leqslant L \tag{38}$$

The rank of $\boldsymbol{C}$ will be *smaller* than L if there exists a linear relationship between some of the partial holograms $\boldsymbol{p}_l$. As a simple example assume two independent partial sources producing corresponding partial holograms which are identical apart from a complex factor. This occurs for example when a vibrational mode of a structure is excited by two independent internal sources.

More precisely, the expression (35) for $\boldsymbol{C}$ shows that the rank I of $\boldsymbol{C}$ is equal to the number of linearly independent partial holograms $\boldsymbol{p}_l$. For any J greater than or equal to the number I of linearly independent partial holograms $\boldsymbol{p}_l$, there exists a matrix $\boldsymbol{A}$ with J columns and N rows such that $\boldsymbol{A}$ can replace $\boldsymbol{P}$ in formula (35):

$$\boldsymbol{A} \equiv \left[\, \boldsymbol{a}_1 \;\; \boldsymbol{a}_2 \;\; \ldots \;\; \boldsymbol{a}_J \,\right] \tag{39}$$

$$\boldsymbol{C} = \boldsymbol{A}^{\star}\, \boldsymbol{A}^{T} \tag{40}$$

The columns $\boldsymbol{a}_i$ of $\boldsymbol{A}$ shall be denoted as composite holograms, and the matrix $\boldsymbol{A}$ shall be said to represent $\boldsymbol{C}$. Each composite hologram $\boldsymbol{a}_i$ is a linear combination of the partial holograms $\boldsymbol{p}_l$. For $J = I$ the matrix $\boldsymbol{A}$ constitutes a minimum representation of the cross spectrum hologram matrix $\boldsymbol{C}$.

It can be easily verified that the linear combinations of $\boldsymbol{p}_l$, constituting the columns $\boldsymbol{a}_i$ of $\boldsymbol{A}$, are not unique. To show this, let $\boldsymbol{A}$ be a particular representation of $\boldsymbol{C}$, $\boldsymbol{C} = \boldsymbol{A}^{\star}\, \boldsymbol{A}^{T}$, and let $\boldsymbol{W}$ be any J by J orthonormal matrix, $\boldsymbol{W}^{\star} \boldsymbol{W}^{T} = \boldsymbol{W}^{T}\, \boldsymbol{W}^{\star} = \boldsymbol{I}$, $\boldsymbol{I}$ being unit diagonal. Then the matrix $\boldsymbol{A}\boldsymbol{W}$ is also a valid representation of $\boldsymbol{C}$ because $\boldsymbol{A}^{\star} \boldsymbol{A}^{T} = (\boldsymbol{A}\, \boldsymbol{W})^{\star} (\boldsymbol{A}\, \boldsymbol{W})^{T}$. The representation $\boldsymbol{A}$ that is actually obtained in a specific application will depend strongly upon the method applied to achieve it.

For $J > I$ the matrix $\boldsymbol{W}$ may be selected in a way such that up to J–I columns of $\boldsymbol{A}\boldsymbol{W}$ contain only zeros. Such columns may be removed, causing an effective reduction of J.

3.2. Cross spectral formulation of HIE and NAH

The subsequent section 3.3 gives a detailed discussion of the representation (40) of $\boldsymbol{C}$ in terms of composite holograms $\boldsymbol{a}_i$ and a description of an

efficient technique to obtain such a representation. At this point we proceed to the formulation of NAH in connection with the cross spectral description of the sound field.

Based on the representations (35) and (36) of $\boldsymbol{C}$ and $\tilde{\boldsymbol{C}}$ in terms of complex time harmonic pressure fields which are mutually uncorrelated, we can apply the matrix formulation of the NAH and HIE propagation tools described previously. Application of the NAH transform formula (20) in connection with partial hologram $\boldsymbol{p}_l$ from independent partial source no. l yields

$$\tilde{\boldsymbol{p}}_l = \boldsymbol{H}\boldsymbol{p}_l \qquad l = 1, 2, ..., L \tag{41}$$

Since the column matrices $\boldsymbol{p}_l$ and $\tilde{\boldsymbol{p}}_l$ constitute the columns of the matrices $\boldsymbol{P}$ and $\tilde{\boldsymbol{P}}$, respectively, we conclude from eq. (41) that

$$\tilde{\boldsymbol{P}} = \boldsymbol{H}\boldsymbol{P} \tag{42}$$

From eq. (42) and the expressions (35) and (36) for $\boldsymbol{C}$ and $\tilde{\boldsymbol{C}}$ we now obtain

$$\begin{aligned} \tilde{\boldsymbol{C}} &= \tilde{\boldsymbol{P}}^{\star}\tilde{\boldsymbol{P}}^{T} \\ &= \boldsymbol{H}^{\star}\boldsymbol{P}^{\star}\boldsymbol{P}^{T}\boldsymbol{H}^{T} \\ &= \boldsymbol{H}^{\star}\left(\boldsymbol{P}^{\star}\boldsymbol{P}^{T}\right)\boldsymbol{H}^{T} \\ &= \boldsymbol{H}^{\star}\boldsymbol{C}\,\boldsymbol{H}^{T} \end{aligned} \tag{43}$$

The derived transform formula

$$\tilde{\boldsymbol{C}} = \boldsymbol{H}^{\star}\boldsymbol{C}\,\boldsymbol{H}^{T} \tag{44}$$

is seen to be independent of the number of and the individual forms of the uncorrelated partial fields. It expresses, how the NAH transform tool can be applied in connection with a cross spectral representation of an arbitrary monochromatic sound field.

The cross spectral transform formula (44) could also be derived directly based on the fact that the cross spectrum $C(\underline{r}, \underline{s})$ between positions $\underline{r}$ and $\underline{s}$ satisfies the homogeneous wave equation (1) in both spatial variables $\underline{r}$ and $\underline{s}$, [1]. Thus, $C(\underline{r}, \underline{s})$ can be transformed from one plane to another by transformation in the two spatial variables $\underline{r}$ and $\underline{s}$ independently, corresponding to the pre-multiplication with $\boldsymbol{H}^{\star}$ and the post-multiplication with $\boldsymbol{H}^{T}$ in eq. (44).

Since in practice we do not actually measure or calculate the large cross spectrum hologram matrix $\boldsymbol{C}$, but rather use a representation in terms of a matrix $\boldsymbol{A}$ of composite holograms, the NAH transform tool should be formulated for application in connection with the representation $\boldsymbol{A}$.

Substitution of the representation formula (40) in the cross spectral transform formula (44) leads to

$$\begin{aligned}\tilde{\boldsymbol{C}} &= \boldsymbol{H}^{\star}\boldsymbol{C}\ \boldsymbol{H}^{T} \\ &= \boldsymbol{H}^{\star}\boldsymbol{A}^{\star}\boldsymbol{A}^{T}\boldsymbol{H}^{T} \\ &= (\boldsymbol{H}\ \boldsymbol{A})^{\star}(\boldsymbol{H}\ \boldsymbol{A})^{T}\end{aligned} \tag{45}$$

Clearly, if we define the transformed representation $\tilde{\boldsymbol{A}}$ as

$$\tilde{\boldsymbol{A}} \equiv \boldsymbol{H}\ \boldsymbol{A} \tag{46}$$

then the cross spectrum output matrix becomes

$$\tilde{\boldsymbol{C}} = \tilde{\boldsymbol{A}}^{\star}\tilde{\boldsymbol{A}}^{T} \tag{47}$$

Note that the columns $\tilde{\boldsymbol{a}}_i$ of $\tilde{\boldsymbol{A}}$ are simply the transformed composite holograms: $\tilde{\boldsymbol{a}}_i = \boldsymbol{H}\boldsymbol{a}_i$. By comparing eqs. (46) and (47) with eqs. (42) and (36) it is evident that we can transform the composite hologram representation $\boldsymbol{A}$ exactly as if it were a true partial hologram representation $\boldsymbol{P}$, as long as we are interested only in calculating parts of the output cross spectrum matrix $\tilde{\boldsymbol{C}}$ for the total sound field. In other words, we can transform the composite holograms $\boldsymbol{a}_i$ as if each one of them represented a complex time harmonic sound field, although we know that in general each one of them represents a linear combination of uncorrelated complex time harmonic fields. However, it should be recalled that these properties have been derived based on the assumption that the set of composite holograms $\boldsymbol{a}_i$ fully represent the cross spectrum hologram matrix $\boldsymbol{C}$, ref. eq. (40).

Considering the non-uniqueness of the representation $\boldsymbol{A}$, it is evident from eqs. (46) and (47) that substitution of $\boldsymbol{A}\boldsymbol{W}$ for $\boldsymbol{A}$ does not influence the result $\tilde{\boldsymbol{C}}$, the matrix $\boldsymbol{W}$ being orthonormal, $\boldsymbol{W}^{\star}\boldsymbol{W}^{T} = \boldsymbol{W}^{T}\boldsymbol{W}^{\star} = \boldsymbol{I}$. The calculated output matrix $\tilde{\boldsymbol{C}}$ therefore does not depend on which representation, $\boldsymbol{A}$, one has obtained.

For normal applications, only the diagonal of $\tilde{\boldsymbol{C}}$ will be calculated from $\tilde{\boldsymbol{A}}$. The diagonal contains the autospectra at the output grid positions, while the off-diagonal elements of $\tilde{\boldsymbol{C}}$ are the cross spectra between these grid points. The autospectra allow the sound pressure and the acoustic potential energy to be calculated.

Having discussed in detail the application of NAH for a simple plane to plane transformation of a cross spectral sound field description, we proceed to the problem of obtaining the other acoustical descriptors such as sound intensity, particle velocity and acoustic kinetic energy in the output plane.

Also here we shall need the representation $\boldsymbol{P}$ of the cross spectrum hologram matrix $\boldsymbol{C}$ in terms of complex time harmonic partial fields for the derivations.

Considering the partial hologram representation $\boldsymbol{P}$, then for each of the partial holograms $\boldsymbol{p}_l$ we can apply the NAH propagator $\boldsymbol{H}_u$ of eq. (24) to obtain the corresponding particle velocity distribution $\tilde{\boldsymbol{u}}_l$ in the output plane. Defining the matrix $\tilde{\boldsymbol{U}}$ of partial field particle velocity distributions in the output plane as

$$\tilde{\boldsymbol{U}} = \left[\tilde{\boldsymbol{u}}_1 \, \tilde{\boldsymbol{u}}_2 \, \ldots \, \tilde{\boldsymbol{u}}_L \right] \tag{48}$$

then the transform (23) of all the partial holograms can be written in the compact matrix form

$$\tilde{\boldsymbol{U}} = \boldsymbol{H}_u \, \boldsymbol{P} \tag{49}$$

corresponding to eq. (42) for the matrix $\tilde{\boldsymbol{P}}$ of partial pressure fields in the output plane.

Instead of the pressure/pressure output cross spectrum matrix $\tilde{\boldsymbol{C}}$, we shall now consider the pressure/particle-velocity output cross spectrum matrix $\tilde{\boldsymbol{C}}_{pu}$ which can be expressed in the following way:

$$\tilde{\boldsymbol{C}}_{pu} = \tilde{\boldsymbol{P}}^{\star} \, \tilde{\boldsymbol{U}}^{T} \tag{50}$$

and the particle-velocity/particle-velocity output cross spectrum matrix $\tilde{\boldsymbol{C}}_{uu}$ given by

$$\tilde{\boldsymbol{C}}_{uu} = \tilde{\boldsymbol{U}}^{\star} \, \tilde{\boldsymbol{U}}^{T} \tag{51}$$

The diagonal of $\tilde{\boldsymbol{C}}_{pu}$ contains full information about active and reactive intensity in the output plane, while $\tilde{\boldsymbol{C}}_{uu}$ provides us with the particle velocity level and the acoustic kinetic energy. We need to show that $\tilde{\boldsymbol{C}}_{pu}$ and $\tilde{\boldsymbol{C}}_{uu}$ can be obtained from the composite hologram representation $\boldsymbol{A}$ of the sound field.

For this we define the matrix $\tilde{\boldsymbol{A}}_u$ of composite field particle velocity distributions in the output plane $\tilde{S}$ as follows:

$$\tilde{\boldsymbol{A}}_u \equiv \boldsymbol{H}_u \, \boldsymbol{A} \tag{52}$$

Application of the formulae (50), (42), (49), (35), (40), (46) and (52) allows the following rewriting of the expression (50) for $\tilde{\boldsymbol{C}}_{pu}$:

$$\begin{aligned}\tilde{\boldsymbol{C}}_{pu} &= \tilde{\boldsymbol{P}}^{\star}\ \tilde{\boldsymbol{U}}^{T} \\ &= \boldsymbol{H}^{\star}\ \boldsymbol{P}^{\star}\ \boldsymbol{P}^{T}\ \boldsymbol{H}_{u}{}^{T} \\ &= \boldsymbol{H}^{\star}\ \boldsymbol{C}\ \boldsymbol{H}_{u}{}^{T} \\ &= \boldsymbol{H}^{\star}\ \boldsymbol{A}^{\star}\ \boldsymbol{A}^{T}\ \boldsymbol{H}_{u}{}^{T} \\ &= \tilde{\boldsymbol{A}}^{\star}\ \tilde{\boldsymbol{A}}_{u}{}^{T}\end{aligned} \tag{53}$$

For a corresponding rewriting of $\tilde{\boldsymbol{C}}_{uu}$ we apply formulae (51), (49), (35), (40) and (52):

$$\begin{aligned}\tilde{\boldsymbol{C}}_{uu} &= \tilde{\boldsymbol{U}}^{\star}\ \tilde{\boldsymbol{U}}^{T} \\ &= \boldsymbol{H}_{u}^{\star}\,\boldsymbol{P}^{\star}\ \boldsymbol{P}^{T}\,\boldsymbol{H}_{u}{}^{T} \\ &= \boldsymbol{H}_{u}^{\star}\,\boldsymbol{C}\ \boldsymbol{H}_{u}{}^{T} \\ &= \boldsymbol{H}_{u}^{\star}\,\boldsymbol{A}^{\star}\ \boldsymbol{A}^{T}\ \boldsymbol{H}_{u}{}^{T} \\ &= \tilde{\boldsymbol{A}}_{u}^{\star}\ \tilde{\boldsymbol{A}}_{u}{}^{T}\end{aligned} \tag{54}$$

The derived expressions (53) and (54) for $\tilde{\boldsymbol{C}}_{pu}$ and $\tilde{\boldsymbol{C}}_{uu}$, respectively, show that these matrices can actually be obtained by application of the standard NAH formulation on the matrix $\boldsymbol{A}$ of composite holograms.

In conclusion, the present section has demonstrated why and how the power and energy descriptors of an arbitrary sound field can be obtained from a set of composite holograms $\boldsymbol{a}_i$ that represent the cross spectrum hologram matrix $\boldsymbol{C}$. In this context, each one of the composite holograms $\boldsymbol{a}_i$ can be treated as if it represented an independent, time harmonic partial field.

3.3. An efficient principal component technique for obtaining a cross spectral sound field representation

The problem to be addressed in the present section will be how to achieve a representation of the cross spectrum hologram matrix $\boldsymbol{C}$ through a minimum of data acquisition. Clearly, direct measurement of the entire matrix $\boldsymbol{C}$ will in general be an enormous task. As an example, a 25×40 measurement grid (hologram grid), defining $N = 1000$ measurement points, would require the measurement of $\frac{1}{2}N(N+1) = 500\,500$ cross spectra, even when advantage is taken of the conjugate symmetry of $\boldsymbol{C}$, $\boldsymbol{C}^{T} = \boldsymbol{C}^{\star}$.

As described in the previous section, we wish to achieve a representation of $\boldsymbol{C}$, $\boldsymbol{C} = \boldsymbol{A}^{\star}\boldsymbol{A}^{T}$, in terms of a matrix $\boldsymbol{A}$, the columns of which are a set of composite holograms $\boldsymbol{a}_i$, $i = 1, 2, \ldots, J$. For this we apply a principal component technique similar to that described in references [15] and [16]. A set of reference transducers provides a set of signals to be considered as

system inputs, while the signals at the hologram grid positions are considered as outputs. The cross spectra between the set of references enable the calculation of a set of principal components created by a set of virtual sources which are linear combinations of the true independent partial sources. The composite holograms $\boldsymbol{a}_i$ created by these virtual sources at the system output shall be denoted as principal holograms, although the principal component expansion is done at the system input.

3.3.1. Measurement employing a set of references

With reference to Fig. 4 we apply again the mathematical model describing the total sound source as consisting of L uncorrelated partial sources producing partial holograms $\boldsymbol{p}_l$, $l = 1, 2, ..., L$, on the measurement plane. Now, we introduce a set (a grid) of K reference transducers, and denote by $\boldsymbol{r}_l$ the K element column matrix of signals from partial source no. l measured by the K reference transducers. The column matrix $\boldsymbol{r}_l$ represents a trace of the signal from partial source no. l over the references. Further-

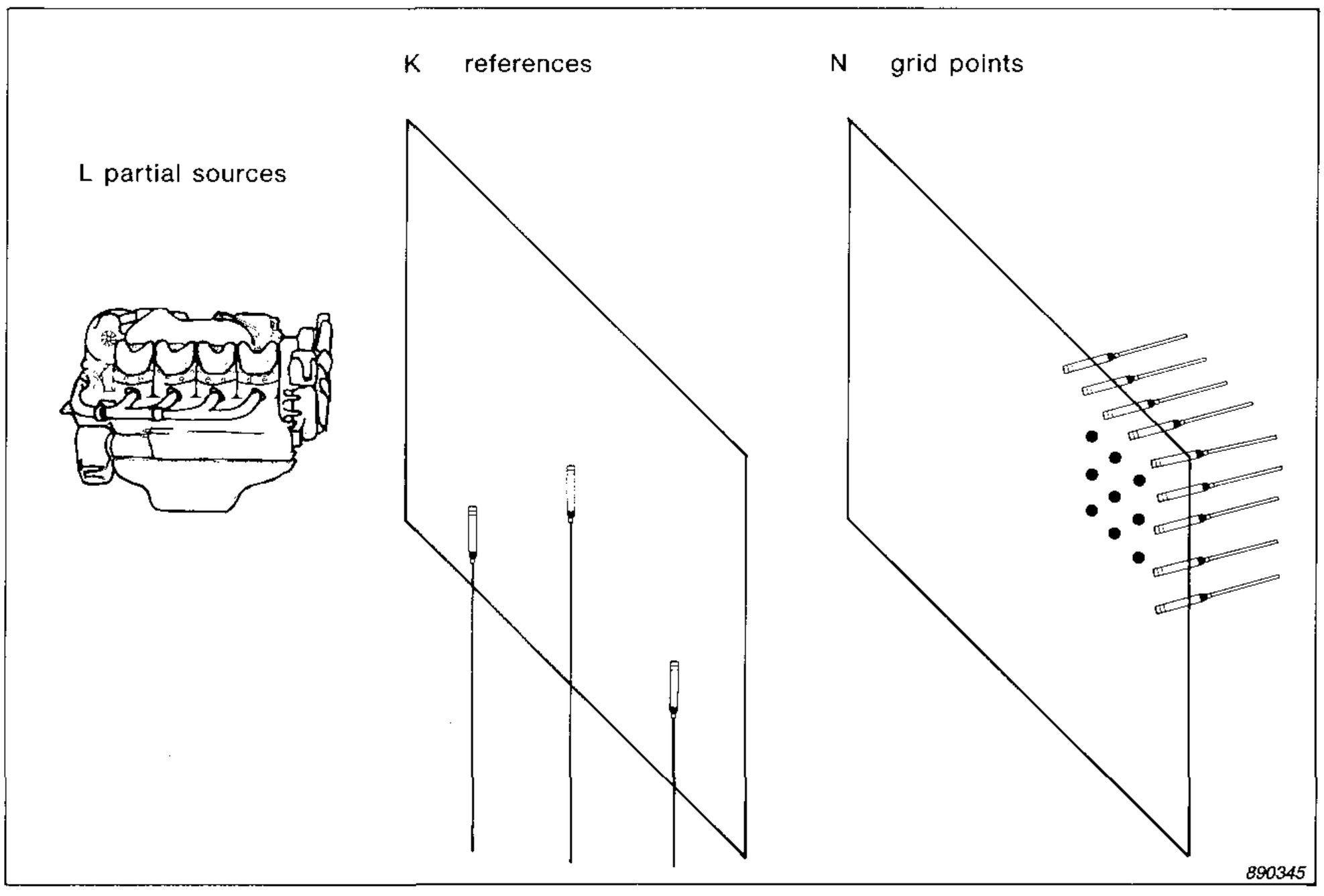

Fig. 4. Schematic representation of sources, references and hologram grid. The references can be positioned arbitrarily and need not be pressure transducers. The geometry is not representative

more, we also introduce a matrix $\boldsymbol{R}$, the columns of which are the reference traces $\boldsymbol{r}_l$, $l = 1, 2, ..., L$, for the partial sources:

$$\boldsymbol{R} \equiv \left[\boldsymbol{r}_1 \ \boldsymbol{r}_2 \ ... \ \boldsymbol{r}_L \right] \tag{55}$$

Each row of $\boldsymbol{R}$ represents the view of the L partial fields as seen from a particular reference.

The measurement and calculation technique for extraction of a representation $\boldsymbol{A}$ is based on a unifying view of the K references and N hologram grid points. For this, we introduce the set of extended partial holograms $\boldsymbol{q}_l$, $l = 1, 2, ..., L$:

$$\boldsymbol{q}_l \equiv \begin{bmatrix} \boldsymbol{r}_l \\ \\ \boldsymbol{p}_l \end{bmatrix} \tag{56}$$

Each extended partial hologram $\boldsymbol{q}_l$ contains the complex signals at the K references and N hologram grid points for the corresponding independent partial source no. l. The extended partial holograms $\boldsymbol{q}_l$ constitute the columns of a matrix $\boldsymbol{Q}$ defined as follows:

$$\boldsymbol{Q} \equiv \left[\boldsymbol{q}_1 \ \boldsymbol{q}_2 \ ... \ \boldsymbol{q}_L \right] = \begin{bmatrix} \boldsymbol{R} \\ \\ \boldsymbol{P} \end{bmatrix} \tag{57}$$

Here $\boldsymbol{R}$ and $\boldsymbol{P}$ are defined in eqs. (55) and (33) respectively.

Having defined the partial source signals at the reference and hologram grid points, we can express the cross spectra between the various measurement positions in terms of these signals. The matrix $\boldsymbol{C}_+$ of cross spectra between the positions of the extended hologram grid (reference grid plus hologram grid) can be expressed as

$$\boldsymbol{C}_+ = \boldsymbol{Q}^\star \boldsymbol{Q}^T \tag{58}$$

which follows from the same arguments as those leading to the corresponding expression (35) for the cross spectrum hologram matrix $\boldsymbol{C}$. The matrix $\boldsymbol{C}_+$ shall be denoted as the extended cross spectrum hologram matrix.

Now, from eqs. (58) and (57) we obtain the following expansion of $\boldsymbol{C}_+$,

$$\boldsymbol{C}_+ = \begin{bmatrix} \boldsymbol{C}_R & \boldsymbol{C}_\Delta \\ \boldsymbol{C}_\Delta{}^{\star T} & \boldsymbol{C} \end{bmatrix} \tag{59}$$

where

$$\boldsymbol{C}_R = \boldsymbol{R}^\star \boldsymbol{R}^T \tag{60}$$

is the reference cross spectrum matrix,

$$\boldsymbol{C}_\Delta = \boldsymbol{R}^\star \boldsymbol{P}^T \tag{61}$$

is the so-called scan cross spectrum matrix containing the cross spectra from the references to the hologram grid points, and

$$\boldsymbol{C} = \boldsymbol{P}^\star \boldsymbol{P}^T \tag{62}$$

is the cross spectrum hologram matrix. Use of these matrices allows the basic principle applied in STSF to obtain a representation of $\boldsymbol{C}$ to be described through the following steps:

1. Measure the reference cross spectrum matrix $\boldsymbol{C}_R$
2. Measure the matrix $\boldsymbol{C}_\Delta$ of cross spectra from the references to the hologram grid points
3. Calculate a representation $\boldsymbol{A}$ of $\boldsymbol{C}$ from the matrices $\boldsymbol{C}_R$ and $\boldsymbol{C}_\Delta$.

3.3.2. Calculation of principal components

The calculation of $\boldsymbol{A}$ mentioned under point 3 above is based on some assumptions about the ranks of the matrices $\boldsymbol{C}_+$, $\boldsymbol{C}_R$ and $\boldsymbol{C}$. Following the discussion around eqs. (37–40), the rank I of $\boldsymbol{C}$ equals the number of linearly independent partial holograms $\boldsymbol{p}_l$ from the set of independent partial sources. Two partial holograms are linearly indepedent if they exhibit different variations in amplitude and phase over the hologram grid. Similarly, the rank of $\boldsymbol{C}_R$ is equal to the number of linearly independent reference traces $\boldsymbol{r}_l$, and the rank of $\boldsymbol{C}_+$ is equal to the number of linearly independent extended partial holograms $\boldsymbol{q}_l$. These statements can be verified from the similar expressions (35), (60) and (58) for the matrices $\boldsymbol{C}$, $\boldsymbol{C}_R$ and $\boldsymbol{C}_+$ respectively.

For the considerations of matrix rank we shall assume that the number K of references is much smaller than the number N of hologram grid points, $K \ll N$.

Since both $\boldsymbol{C}_R$ and $\boldsymbol{C}$ are submatrices of $\boldsymbol{C}_+$, we have

$$\text{rank}\,(\boldsymbol{C}_+) \geqslant \text{rank}\,(\boldsymbol{C}_R) \tag{63}$$

$$\text{rank}\,(\boldsymbol{C}_+) \geqslant \text{rank}\,(\boldsymbol{C}) \tag{64}$$

In terms of the partial fields from the independent partial sources, these inequalities express that neither the number of linearly independent reference traces $\boldsymbol{r}_l$ nor the number of linearly independent partial holograms $\boldsymbol{p}_l$ can exceed the number of linearly independent extended partial holograms $\boldsymbol{q}_l$.

To obtain a complete reconstruction of the cross spectrum hologram matrix $\boldsymbol{C}$ from the measured matrices $\boldsymbol{C}_R$ and $\boldsymbol{C}_\Delta$, we have to assume equal rank of $\boldsymbol{C}_R$ and $\boldsymbol{C}_+$:

$$\text{rank}\,(\boldsymbol{C}_R) \;=\; \text{rank}\,(\boldsymbol{C}_+) \qquad \textit{assumption} \tag{65}$$

Considering the expansion (59) of $\boldsymbol{C}_+$, the first K columns consisting of $\boldsymbol{C}_R$ and $\boldsymbol{C}_\Delta{}^{\star T}$ are assumed to be known from measurements. This part of $\boldsymbol{C}_+$ shall be denoted as $\boldsymbol{C}_1$ while the remaining part consisting of $\boldsymbol{C}_\Delta$ and $\boldsymbol{C}$ shall be denoted $\boldsymbol{C}_2$:

$$\boldsymbol{C}_1 \equiv \begin{bmatrix} \boldsymbol{C}_R \\ \\ \boldsymbol{C}_\Delta{}^{\star T} \end{bmatrix} \tag{66}$$

$$\boldsymbol{C}_2 \equiv \begin{bmatrix} \boldsymbol{C}_\Delta \\ \\ \boldsymbol{C} \end{bmatrix} \tag{67}$$

$$\boldsymbol{C}_+ \;=\; \begin{bmatrix} \boldsymbol{C}_1 & \boldsymbol{C}_2 \end{bmatrix} \tag{68}$$

Based on the expansions (58), (60), (61) and (62) of $\boldsymbol{C}_+$, $\boldsymbol{C}_R$, $\boldsymbol{C}_\Delta$ and $\boldsymbol{C}$ it is shown in Appendix 1 that

$$\text{rank}\,(\boldsymbol{C}_1) \;=\; \text{rank}\,(\boldsymbol{C}_R) \tag{69}$$

Thus, because of our assumption (65) the measured matrix $\boldsymbol{C}_1$ has rank equal to the rank of $\boldsymbol{C}_+$, which means that the columns of $\boldsymbol{C}_2$ are linear combinations of the columns of $\boldsymbol{C}_1$. Consequently there exists a K by N matrix $\boldsymbol{E}$ enabling $\boldsymbol{C}_2$ to be expressed as

$$\boldsymbol{C}_2 \;=\; \boldsymbol{C}_1\;\boldsymbol{E} \tag{70}$$

Substitution of the expressions (66) and (67) for $\boldsymbol{C}_1$ and $\boldsymbol{C}_2$ in equation (70) leads to the following system of linear equations

$$\boldsymbol{C}_\Delta = \boldsymbol{C}_R \boldsymbol{E} \tag{71a}$$

$$\boldsymbol{C} = \boldsymbol{C}_\Delta^{\star T} \boldsymbol{E} \tag{71b}$$

which can be solved for $\boldsymbol{E}$ and $\boldsymbol{C}$:

$$\boldsymbol{E} = \boldsymbol{C}_R^{-1} \boldsymbol{C}_\Delta \tag{72}$$

$$\boldsymbol{C} = \boldsymbol{C}_\Delta^{\star T} \boldsymbol{C}_R^{-1} \boldsymbol{C}_\Delta \tag{73}$$

Equation (73) constitutes the basis for obtaining the cross spectrum hologram matrix $\boldsymbol{C}$ in STSF.

In connection with the inversion of the reference cross spectrum matrix $\boldsymbol{C}_R$, the possible rank deficiency of this matrix must be taken into account. In general the inverse matrix $\boldsymbol{C}_R^{-1}$ must be replaced by a so-called generalized inverse $\boldsymbol{C}_R^{+}$. This matrix is defined on the basis of an eigenvector expansion of $\boldsymbol{C}_R$,

$$\boldsymbol{C}_R = \boldsymbol{S}^\star \boldsymbol{D} \boldsymbol{S}^T = \sum_{i=1}^{K} d_i \boldsymbol{s}_i^\star \boldsymbol{s}_i^T \tag{74}$$

where $\boldsymbol{D}$ is K by K diagonal with the real, non-negative eigenvalues on the diagonal,

$$\boldsymbol{D} \equiv \begin{bmatrix} d_1 & & & & 0 \\ & d_2 & & & \\ & & \ddots & & \\ & & & d_J & \\ & & & & 0 \\ & & & & & \ddots \\ 0 & & & & & & 0 \end{bmatrix} \tag{75}$$

$\boldsymbol{S}$ is K by K orthonormal,

$$\boldsymbol{S}^\star \boldsymbol{S}^T = \boldsymbol{S}^T \boldsymbol{S}^\star = \boldsymbol{I}_K \tag{76}$$

$\boldsymbol{I}_K$ being the K by K unit diagonal matrix, and $\boldsymbol{s}_i$, $i = 1, 2, \ldots, K$, are the columns of $\boldsymbol{S}$:

$$\boldsymbol{S} = \left[\boldsymbol{s}_1 \ \boldsymbol{s}_2 \ldots \boldsymbol{s}_K \right] \tag{77}$$

In eq. (75) d_i, $i = 1, 2, \ldots, J$, are the non-zero eigenvalues of $\boldsymbol{C}_R$ in descending order. Thus, J is now defined as the rank of $\boldsymbol{C}_R$:

$$J \equiv \text{rank}\,(\boldsymbol{C}_R) = \text{rank}\,(\boldsymbol{C}_+) \geqslant \text{rank}\,(\boldsymbol{C}) = I \tag{78}$$

Defining the generalized inverse $\boldsymbol{D}^+$ of $\boldsymbol{D}$ as

$$\boldsymbol{D}^+ \equiv \begin{bmatrix} d_1^{-1} & & & & & 0 \\ & d_2^{-1} & & & & \\ & & \ddots & & & \\ & & & d_J^{-1} & & \\ & & & & 0 & \\ 0 & & & & & 0 \end{bmatrix} \tag{79}$$

the generalized inverse $\boldsymbol{C}_R{}^+$ of $\boldsymbol{C}_R$ is given the following definition:

$$\boldsymbol{C}_R^+ \equiv \boldsymbol{S}^\star\, \boldsymbol{D}^+\, \boldsymbol{S}^T \tag{80}$$

From eqs. (74–80) it is easy to verify that $\boldsymbol{C}_R\, \boldsymbol{C}_R{}^+ = \boldsymbol{I}_K$ when $\boldsymbol{C}_R$ has full rank, i.e. when $J = K$. In that case $\boldsymbol{C}_R{}^+$ is a true inverse of $\boldsymbol{C}_R$. Otherwise $\boldsymbol{C}_R{}^+$ is inverse to $\boldsymbol{C}_R$ only in the subspace spanned by the first J columns of $\boldsymbol{S}$. In the so-called zero-subspace spanned by the last $(K-J)$ columns no inverse exists.

To show that the cross spectrum matrix $\boldsymbol{C}$ is uniquely defined by eq. (73) despite the presence of a zero-subspace, we introduce a matrix $\boldsymbol{S}_1$ containing the first J columns of $\boldsymbol{S}$,

$$\boldsymbol{S}_1 \equiv \left[\boldsymbol{s}_1\ \boldsymbol{s}_2\ \ldots\ \boldsymbol{s}_J\right] \tag{81}$$

and a matrix $\boldsymbol{S}_2$ consisting of the remaining $(K-J)$ columns:

$$\boldsymbol{S}_2 \equiv \left[\boldsymbol{s}_{J+1}\ \boldsymbol{s}_{J+2}\ \ldots\ \boldsymbol{s}_K\right] \tag{82}$$

Thus $\boldsymbol{S}$ can be written as

$$\boldsymbol{S} = \left[\boldsymbol{S}_1\ \boldsymbol{S}_2\right] \tag{83}$$

and since the columns of $\boldsymbol{S}$ are orthogonal, we have

$$\boldsymbol{S}_1{}^T\, \boldsymbol{S}_2^\star = \boldsymbol{S}_2^T\, \boldsymbol{S}_1^\star = \boldsymbol{O} \tag{84}$$

Similarly, we introduce a J by J diagonal matrix $\boldsymbol{D}_1$ containing the J non-zero eigenvalues d_i, $i = 1, 2, \ldots, J$, of $\boldsymbol{C}_R$:

$$\boldsymbol{D}_1 \equiv \begin{bmatrix} d_1 & & & 0 \\ & d_2 & & \\ & & \ddots & \\ 0 & & & d_J \end{bmatrix} \tag{85}$$

The complete eigenvalue matrix $\boldsymbol{D}$ defined in eq. (75) can then be written as

$$\boldsymbol{D} = \begin{bmatrix} \boldsymbol{D}_1 & \boldsymbol{O} \\ \boldsymbol{O} & \boldsymbol{O} \end{bmatrix} \tag{86}$$

and from eq. (79) it is evident that the generalized inverse $\boldsymbol{D}^+$ of $\boldsymbol{D}$ can be expressed in the following way:

$$\boldsymbol{D}^+ = \begin{bmatrix} \boldsymbol{D}_1^{-1} & \boldsymbol{O} \\ \boldsymbol{O} & \boldsymbol{O} \end{bmatrix} \tag{87}$$

Using the subdivisions of $\boldsymbol{S}$, $\boldsymbol{D}$ and $\boldsymbol{D}^+$ given above, the eigenvector expansions (74) and (80) of $\boldsymbol{C}_R$ and $\boldsymbol{C}_R{}^+$ can be reduced to

$$\boldsymbol{C}_R = \boldsymbol{S}_1^{\star}\, \boldsymbol{D}_1\, \boldsymbol{S}_1^T = \sum_{i=1}^{J} d_i\, \boldsymbol{s}_i^{\star} \boldsymbol{s}_i^T \tag{88}$$

$$\boldsymbol{C}_R^+ = \boldsymbol{S}_1^{\star}\, \boldsymbol{D}_1^{-1} \boldsymbol{S}_1^T = \sum_{i=1}^{J} d_i^{-1}\, \boldsymbol{s}_i^{\star} \boldsymbol{s}_i^T \tag{89}$$

Consider now the original system of linear equations (71) assuming $\boldsymbol{C}$, $\boldsymbol{C}_\Delta$ and $\boldsymbol{C}_R$ to be known. Denoting by $\boldsymbol{E}_0$ a solution to eqs. (71), then because of the expression (88) for $\boldsymbol{C}_R$ and the orthogonality (84) between $\boldsymbol{S}_1$ and $\boldsymbol{S}_2$ any matrix of the form

$$\boldsymbol{E} = \boldsymbol{E}_0 + \boldsymbol{S}_2^{\star} \boldsymbol{X} \tag{90}$$

will also be a solution to eq. (71a), $\boldsymbol{X}$ being any $(K-J)$ by N complex matrix. To test if $\boldsymbol{E} = \boldsymbol{E}_0 + \boldsymbol{S}_2^{\star}\boldsymbol{X}$ is a solution also to eq. (71b), we substitute $\boldsymbol{E}_0 + \boldsymbol{S}_2^{\star}\boldsymbol{X}$ for $\boldsymbol{E}$ in this equation. Subsequent application of eq. (71a) with $\boldsymbol{E} = \boldsymbol{E}_0 + \boldsymbol{S}_2^{\star}\boldsymbol{X}$ and the eigenvector expansion (88) of $\boldsymbol{C}_R$ leads to the following test equation:

$$\boldsymbol{C} = \left(\boldsymbol{E}_0{}^{\star T} + \boldsymbol{X}^{\star T} \boldsymbol{S}_2^T \right) \boldsymbol{S}_1^{\star}\, \boldsymbol{D}_1\, \boldsymbol{S}_1^T \left(\boldsymbol{E}_0 + \boldsymbol{S}_2^{\star} \boldsymbol{X} \right) \tag{91}$$

Since $\boldsymbol{S}_1$ and $\boldsymbol{S}_2$ are orthogonal, the terms including $\boldsymbol{X}$ cancel, and we conclude that $\boldsymbol{E} = \boldsymbol{E}_0 + \boldsymbol{S}_2^{\star}\boldsymbol{X}$ is a solution also to eq. (71b). Use of $\boldsymbol{C}_R{}^{+}$ for $\boldsymbol{C}_R{}^{-1}$ in eq. (72) means that we select a particular solution $\boldsymbol{E}_0$ for $\boldsymbol{E}$ between the infinity of possible solutions. However, since eq. (71b) holds for all of these possible solutions, we obtain the correct matrix $\boldsymbol{C}$ when eq. (71b) is used to obtain $\boldsymbol{C}$, no matter which solution $\boldsymbol{E}_0$ we have obtained for $\boldsymbol{E}$.

Substitution of $\boldsymbol{C}_R{}^{+}$ for $\boldsymbol{C}_R{}^{-1}$ in the expression (73) for the cross spectrum hologram matrix $\boldsymbol{C}$ leads to

$$\begin{aligned}\boldsymbol{C} &= \boldsymbol{C}_{\Delta}{}^{\star T}\,\boldsymbol{S}^{\star}\boldsymbol{D}^{+}\,\boldsymbol{S}^{T}\,\boldsymbol{C}_{\Delta} \\ &= \boldsymbol{C}_{\Delta}{}^{\star T}\,\boldsymbol{S}_1^{\star}\,\boldsymbol{D}_1^{-1}\,\boldsymbol{S}_1^{T}\,\boldsymbol{C}_{\Delta} \\ &= \left(\boldsymbol{C}_{\Delta}^{T}\boldsymbol{S}_1\,\boldsymbol{D}_1{}^{-1/2}\right)^{\star}\,\left(\boldsymbol{C}_{\Delta}^{T}\boldsymbol{S}_1\,\boldsymbol{D}_1{}^{-1/2}\right)^{T}\end{aligned} \tag{92}$$

where the eigenvector expansion (89) for $\boldsymbol{C}_R{}^{+}$ has been used. In eq. (92) $\boldsymbol{D}_1{}^{-1/2}$ is a J by J diagonal matrix with the numbers $d_i{}^{-1/2}$, $i = 1, 2, \ldots, J$, on the diagonal.

A quasi-minimum representation $\boldsymbol{A}$ of $\boldsymbol{C}$ can now be achieved by defining

$$\boldsymbol{A} \equiv \boldsymbol{C}_{\Delta}^{T}\;\boldsymbol{S}_1\,\boldsymbol{D}_1{}^{-1/2} \tag{93}$$

which can be split up in expressions for the principal holograms constituting the columns of $\boldsymbol{A}$:

$$\boldsymbol{a}_i = d_i{}^{-1/2}\,\boldsymbol{C}_{\Delta}{}^{T}\,\boldsymbol{s}_i \qquad\qquad i = 1, 2, \ldots, J \tag{94}$$

Clearly, because of eqs. (92–93) we have $\boldsymbol{C} = \boldsymbol{A}^{\star}\,\boldsymbol{A}^{T}$ as required, see for example equation (40). Notice that the matrix $\boldsymbol{A}$ defined in eq. (93) has J columns instead of I, and therefore it does not constitute a minimum representation when $J > I$. This is due to the fact that the principal components are defined at the system input (the references).

In practice, however, the matrix ranks (the number of non-zero eigenvalues) are not as well defined as stated in the foregoing treatment. The number of non-zero eigenvalues will always have to be determined by introduction of some threshold level. Further, the rank J of the reference cross spectrum matrix $\boldsymbol{C}_R$ will often be smaller than the actual rank of the extended cross spectrum hologram matrix $\boldsymbol{C}_+$, violating the assumption (65). We shall therefore consider the errors introduced in $\boldsymbol{C}$ by application of the representation $\boldsymbol{A}$ defined in eq. (93) in connection with an insufficient set of references, i.e. a set of references causing the rank of $\boldsymbol{C}_R$ to be smaller than the rank of $\boldsymbol{C}_+$.

3.3.3. Error analysis for insufficient reference sets

To express mathematically the implications of using an insufficient set of references, we need to use again the model representing the total sound field as a set of complex time harmonic partial fields from a corresponding set of mutually uncorrelated partial sources. In other words, we assume that the cross spectrum matrices $\boldsymbol{C}_R$, $\boldsymbol{C}_\perp$ and $\boldsymbol{C}$ can be expressed as in eqs. (60), (61) and (62) respectively.

The partial field model expresses the reference cross spectrum matrix in terms of a matrix $\boldsymbol{R}$, the columns of which are traces $\boldsymbol{r}_l$ over the reference positions of the field from individual partial sources. For this matrix $\boldsymbol{R}$ we shall need a Singular Value Decomposition (SVD) of the following form:

$$\boldsymbol{R} = \boldsymbol{S}\,\boldsymbol{\Gamma}\,\boldsymbol{V}^T \tag{95}$$

Here, $\boldsymbol{V}$ is L by L orthonormal,

$$\boldsymbol{V}\,\boldsymbol{V}^{\star T} = \boldsymbol{V}^{\star T}\,\boldsymbol{V} = \boldsymbol{I}_L \tag{96}$$

$\boldsymbol{I}_L$ being the L by L unit matrix, $\boldsymbol{\Gamma}$ is K by L diagonal with the singular values γ_i on the diagonal, and $\boldsymbol{S}$ will prove to be the K by K orthonormal matrix appearing also in the eigenvector expansion (74) of $\boldsymbol{C}_R$. The singular values γ_i are real and non-negative, and the number of singular values is equal to the smallest of the numbers K and L, $min\{K, L\}$. The number K of references can be smaller than or larger than the number L of partial sources.

Substitution of eq. (95) in the partial field expression (60) for $\boldsymbol{C}_R$ leads to

$$\begin{aligned}\boldsymbol{C}_R &= \boldsymbol{S}^\star\,\boldsymbol{\Gamma}^\star\boldsymbol{V}^{\star T}\,\boldsymbol{V}\boldsymbol{\Gamma}^T\,\boldsymbol{S}^T \\ &= \boldsymbol{S}^\star\left(\boldsymbol{\Gamma}^\star\,\boldsymbol{\Gamma}^T\right)\boldsymbol{S}^T\end{aligned} \tag{97}$$

showing that we can assume the same matrix $\boldsymbol{S}$ in the expansions (74) and (95) of $\boldsymbol{C}_R$ and $\boldsymbol{R}$ respectively. Further, comparison of eqs. (97) and (74) reveals the following relations

$$\boldsymbol{D} = \boldsymbol{\Gamma}^\star\boldsymbol{\Gamma}^T \tag{98a}$$

$$d_i = \gamma_i^\star\gamma_i = \gamma_i^2 \qquad i = 1,2,\ldots,min\{K, L\} \tag{98b}$$

where eq. (98b) expresses the implications of eq. (98a) for the diagonal elements of the two diagonal matrices $\boldsymbol{D}$ and $\boldsymbol{\Gamma}$. If K is larger than L, then we have $d_i = 0$ for $i > L$, and since both d_i and γ_i are real and non-negative, eq. (98b) implies that $\gamma_i = \sqrt{d_i} = d_i^{1/2}$.

Now, following the expression (75) for $\boldsymbol{D}$ only the first J diagonal elements d_i are different from zero, J being the rank of $\boldsymbol{C}_R$. Thus, according to eq. (98b), J cannot exceed $min\{K, L\}$, and only the first J diagonal elements γ_i of $\boldsymbol{\Gamma}$ are non-zero, which reflects the fact that $\boldsymbol{C}_R$ and $\boldsymbol{R}$ have the same rank J because of their mutual relation (60).

Since only the first J diagonal elements γ_i of $\boldsymbol{\Gamma}$ are non-zero, the SVD of $\boldsymbol{R}$ in eq. (95) can be rewritten in the following way

$$\boldsymbol{R} = \boldsymbol{S}\,\boldsymbol{\Gamma}\,\boldsymbol{V}^T = \sum_{i=1}^{J} \gamma_i \boldsymbol{s}_i \boldsymbol{v}_i^T \tag{99}$$

where $\boldsymbol{s}_i$, $i = 1, 2, ..., K$, are the columns of $\boldsymbol{S}$ and $\boldsymbol{v}_i$, $i = 1, 2, ..., L$, are the columns of $\boldsymbol{V}$. Apparently the first J columns $\boldsymbol{s}_i$ of $\boldsymbol{S}$ span the columns of $\boldsymbol{R}$ while the first J columns $\boldsymbol{v}_i$ of $\boldsymbol{V}$ span the rows of $\boldsymbol{R}$.

Since the columns $\boldsymbol{r}_l$ of $\boldsymbol{R}$ are traces of the individual partial fields over the reference positions, the columns $\boldsymbol{s}_i$ of $\boldsymbol{S}$ constitute a set of orthonormal vectors spanning the K-dimensional complex space of possible traces over K references. The singular value γ_i represents the total degree of presence of the unit trace $\boldsymbol{s}_i$ in the traces $\boldsymbol{r}_l$ of the L partial fields.

Similarly, the columns $\boldsymbol{v}_i$ of $\boldsymbol{V}$ constitute a set of orthonormal vectors spanning the L-dimensional complex space of possible views of L different coherent partial fields. The singular value γ_i represents the total degree of presence of the unit view $\boldsymbol{v}_i$ in the views seen from the K references.

From the fact that only the first J singular values γ_i are non-zero, we conclude that only the first J unit views $\boldsymbol{v}_i$, $i = 1, 2, ..., J$, are seen from the K references. These views $\boldsymbol{v}_i$ shall be denoted as the principal views. Similarly, only the first J unit traces $\boldsymbol{s}_i$, $i = 1, 2, ..., J$, which shall be denoted as the principal traces, are covered by the L partial fields.

It should be noted that the principal traces $\boldsymbol{s}_i$ can be achieved through measurement of the reference cross spectrum matrix $\boldsymbol{C}_R$ followed by an eigenvector expansion of this matrix, whereas the principal views $\boldsymbol{v}_i$ are defined only in connection with a set of partial sources and related partial fields. Usually the true partial sources and partial fields are not known. However, the concept of principal views will prove to be a useful tool in understanding the importance and implications of reference selection in the STSF cross spectral technique.

Denote by $\boldsymbol{C}'$ the approximation to the true cross spectrum hologram matrix $\boldsymbol{C}$ obtained by application of the representation $\boldsymbol{A}$ defined in eq. (93) without requiring the matrix rank condition (65) to be fulfilled. Then $\boldsymbol{C}'$ can be expressed as

$$\boldsymbol{C}' \equiv \boldsymbol{A}^{\star}\boldsymbol{A}^{T} \tag{100}$$

where the matrix $\boldsymbol{A}$ is defined in eq. (93). Substitution of the expression (61) for $\boldsymbol{C}_{\lrcorner}$ in eq. (93) followed by substitution of the singular value decomposition (95) for $\boldsymbol{R}$ leads to the formula

$$\boldsymbol{A} = \boldsymbol{P}\,\boldsymbol{V}^{\star}\boldsymbol{\Gamma}^{\star T}\;\boldsymbol{S}^{\star T}\boldsymbol{S}_1\,\boldsymbol{D}_1^{\,1/2} \tag{101}$$

This expression for $\boldsymbol{A}$ can be reduced by application of formulae (83–84) and (98b) with the following result

$$\boldsymbol{A} \;=\; \boldsymbol{P}\;\boldsymbol{V}^{\star}\begin{bmatrix} \boldsymbol{I}_J \\ \\ \boldsymbol{O} \end{bmatrix} \tag{102}$$

where $\boldsymbol{I}_J$ is the J by J unit diagonal matrix.

In order to achieve further reduction in the expression (102), we introduce a subdivision of the orthonormal matrix $\boldsymbol{V}$. The first J columns constituting the principal views are arranged in a matrix $\boldsymbol{V}_1$

$$\boldsymbol{V}_1 \;\equiv\; \left[\boldsymbol{v}_1\;\boldsymbol{v}_2\;\ldots\;\boldsymbol{v}_J\right] \tag{103}$$

and the remaining $(L–J)$ columns in another matrix $\boldsymbol{V}_2$:

$$\boldsymbol{V}_2 \;\equiv\; \left[\boldsymbol{v}_{J+1}\;\boldsymbol{v}_{J+2}\;\ldots\;\boldsymbol{v}_L\right] \tag{104}$$

Thus $\boldsymbol{V}$ can be written as

$$\boldsymbol{V} \;=\; \left[\boldsymbol{V}_1\;\boldsymbol{V}_2\right] \tag{105}$$

The columns of $\boldsymbol{V}_1$ span the subspace of views of the L partial fields that are seen from the set of K references. $\boldsymbol{V}_2$ contains the views that are not seen from the references and perhaps do not exist for the particular set of L partial fields.

Substitution of the subdivision (105) of $\boldsymbol{V}$ in the formula (102) for $\boldsymbol{A}$ leads to the simple expression

$$\boldsymbol{A} \;=\; \boldsymbol{P}\;\boldsymbol{V}_1^{\star} \tag{106}$$

which can be split up in expressions for the principal holograms $\boldsymbol{a}_i$ constituting the columns of $\boldsymbol{A}$:

$$\boldsymbol{a}_i \;=\; \boldsymbol{P}\;\boldsymbol{v}_i^{\star} \qquad\qquad i \;=\; 1, 2, \ldots, J \tag{107}$$

Equation (107) shows that each principal hologram $\boldsymbol{a}_i$ is equal to the projection of the views from the hologram grid positions onto the corresponding principal view $\boldsymbol{v}_i$ from the set of references. Consequently, the part of the total sound field that is represented in $\boldsymbol{A}$ and therefore in $\boldsymbol{C}'$ can be understood as the total views from the hologram grid positions (the rows of $\boldsymbol{P}$) projected onto the subspace of views seen from the references. This subspace is spanned by the principal views $\boldsymbol{v}_i$ constituting the columns of $\boldsymbol{V}_1$.

In relation to eq. (107) notice that the projection vectors $\boldsymbol{v}_i$ define the principal holograms $\boldsymbol{a}_i$ as complex linear combinations of the partial holograms $\boldsymbol{p}_l$ constituting the columns of $\boldsymbol{P}$. The phases of the individual complex weights in $\boldsymbol{v}_i$ reflect the non-physical absolute phases assigned to each of the partial fields and mentioned in connection with eq. (33). From the singular value decomposition (99) of $\boldsymbol{R}$ one may verify that multiplication by a phase factor $e^{j\phi}$ on partial field no. ℓ (column no. ℓ in $\boldsymbol{R}$) introduces the same phase factor $e^{j\phi}$ on weight no. ℓ in all of the unit views $\boldsymbol{v}_l$ constituting the columns of $\boldsymbol{V}$. However, since the phase factor $e^{j\phi}$ on partial field no. ℓ must be introduced also on the partial hologram $\boldsymbol{p}_\ell$ constituting column no. ℓ in $\boldsymbol{P}$, equation (107) shows that the principal holograms $\boldsymbol{a}_i$ are unaffected by such phase factors on the partial fields.

A formula relating the estimated and the true cross spectrum hologram matrices $\boldsymbol{C}'$ and $\boldsymbol{C}$ can be derived from eqs. (62), (100) and (106) by application of the orthonormality relation (96) for $\boldsymbol{V}$ and the subdivision formula (105) for $\boldsymbol{V}$:

$$\begin{aligned}
\boldsymbol{C} &= \boldsymbol{P}^{\star}\ \boldsymbol{P}^{T} \\
&= \boldsymbol{P}^{\star}\left(\boldsymbol{V}\boldsymbol{V}^{\star T}\right)\ \boldsymbol{P}^{T} \\
&= \boldsymbol{P}^{\star}\left(\boldsymbol{V}_1\boldsymbol{V}_1^{\star T} + \boldsymbol{V}_2\boldsymbol{V}_2^{\star T}\right)\ \boldsymbol{P}^{T} \\
&= \boldsymbol{C}' + \left(\boldsymbol{P}\boldsymbol{V}_2^{\star}\right)^{\star}\left(\boldsymbol{P}\boldsymbol{V}_2^{\star}\right)^{T}
\end{aligned} \tag{108}$$

Clearly, the difference between $\boldsymbol{C}$ and $\boldsymbol{C}'$ can be understood as created by the orthogonal projection of the views from the hologram grid onto the subspace of views not seen from the references.

Consequently, in order to obtain a correct estimate $\boldsymbol{C}'$ of the cross spectrum hologram matrix $\boldsymbol{C}$, all the different views of the L partial fields as seen from the set of hologram grid positions must be "spanned" by the set of views from the K references.

On the other hand, the formula (108) relating $\boldsymbol{C}'$ and $\boldsymbol{C}$ also shows that the STSF technique for estimation of $\boldsymbol{C}$ is not very sensitive to violation of the above criterion for a set of references to provide a sufficient set of views

of the total source. This is due to the fact that the part of the total field included in the estimate C' is obtained by an orthogonal projection.

3.3.4. A simple example

As a simple example, consider the measurement setup illustrated in Fig. 5. The main components of the setup are two small loudspeakers and a single reference microphone positioned on the symmetry plane between the two speakers. The two loudspeakers are excited by two identical, independent, narrow-band noise generators which have been adjusted to produce equal sound pressure levels at the reference.

For this measurement setup we have $K = 1$, and since the total sound field can be modelled by two coherent, mutually uncorrelated partial fields — one from each of the two loudspeakers — we have $L = 2$.

Since only one reference is applied, we get only one view of the two partial fields. To define this view we specify arbitrarily that both of the partial fields have phase equal to zero at the reference. Denoting by p the pressure

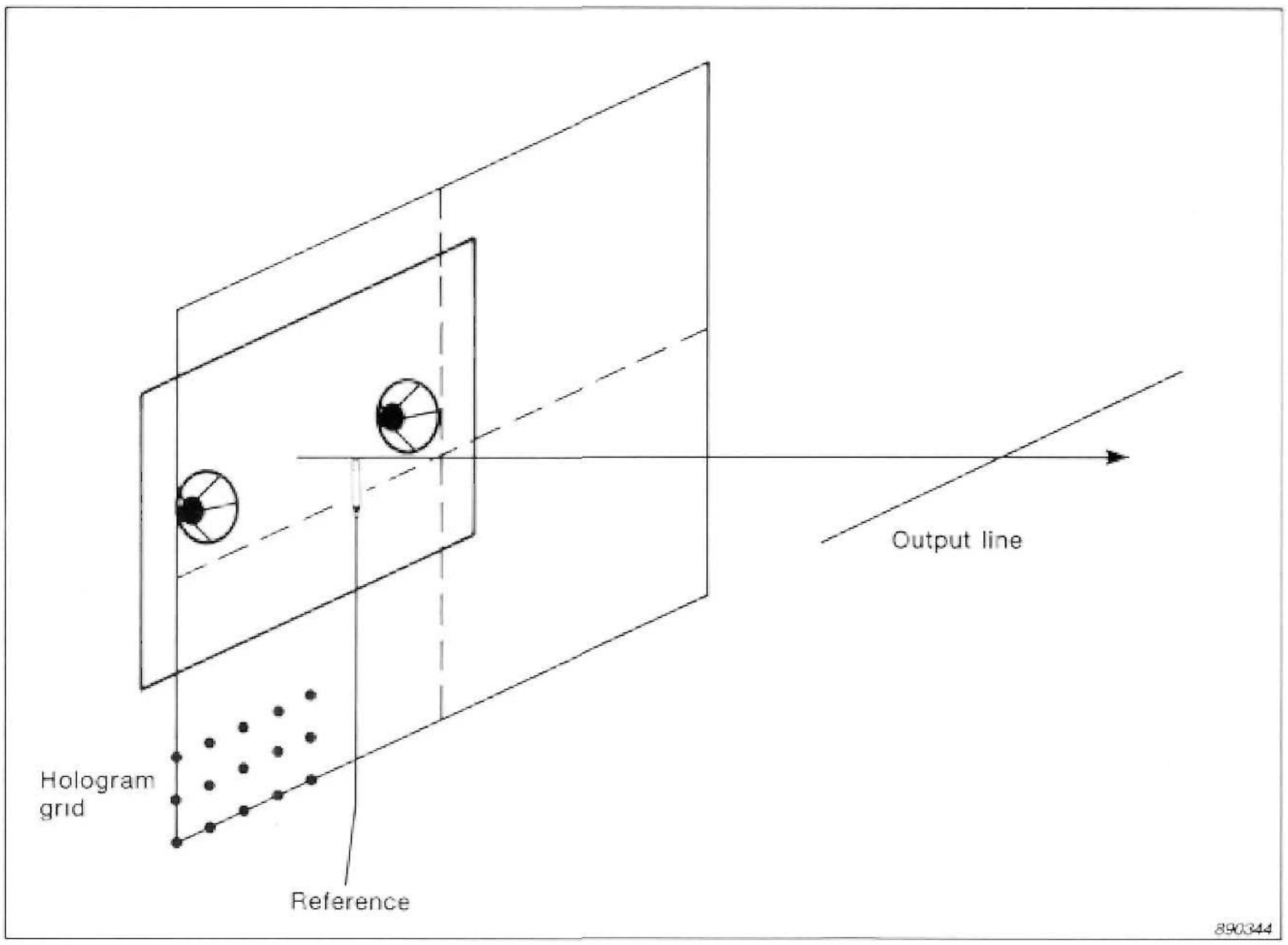

Fig. 5. Measurement setup with two independently excited loudspeakers and one reference

from each of the speakers at the reference position, the matrix $\boldsymbol{R}$ then gets the following simple form

$$\boldsymbol{R} = \begin{bmatrix} p & p \end{bmatrix} = \begin{bmatrix} 1 \end{bmatrix} \begin{bmatrix} \sqrt{2}\,p & 0 \end{bmatrix} \begin{bmatrix} \sqrt{2}/2 & \sqrt{2}/2 \\ \sqrt{2}/2 & -\sqrt{2}/2 \end{bmatrix} \tag{109}$$

where the singular value decomposition of $\boldsymbol{R}$ is also shown. Since we have only one reference view (one row in $\boldsymbol{R}$) there is only one non-zero singular value $\gamma_1 = \sqrt{2}p$. Thus J is equal to one and there is only one principal view $\boldsymbol{v}_1$ constituting the entire matrix $\boldsymbol{V}_1$:

$$\boldsymbol{v}_1 = \begin{bmatrix} \sqrt{2}/2 \\ \sqrt{2}/2 \end{bmatrix} \tag{110}$$

This observation agrees with the fact that the number J of principal views can exceed neither the number K of references nor the number L of partial fields.

The single principal hologram $\boldsymbol{a}_1$ identified by the STSF cross spectral technique can now be expressed in the following way through application of formula (107):

$$\boldsymbol{a}_1 = 1/2\sqrt{2}\,\boldsymbol{p}_1 + 1/2\sqrt{2}\,\boldsymbol{p}_2 \tag{111}$$

Here, $\boldsymbol{p}_1$ and $\boldsymbol{p}_2$ are the partial holograms from each of the two speakers. Recall that the absolute phases of the two partial fields have been (arbitrarily) set to zero at the reference position on the symmetry plane. Consequently, when $\boldsymbol{p}_1$ and $\boldsymbol{p}_2$ are superimposed in amplitude and phase, as prescribed in eq. (111), the sum will equal a hologram created by the two speakers excited in-phase with equal amplitude by a single generator. The principal hologram $\boldsymbol{a}_1$ is equal to the single hologram that would be measured if the two speakers were excited in-phase with amplitude equal to $\sqrt{2}/2$ times the amplitude actually applied.

The results obtained by application of NAH and HIE in connection with the above measurement will reflect the apparent coherent in-phase action of the two speakers. For example the radiation pattern will exhibit strong maxima and minima due to constructive and destructive interference, provided the distance between the speakers is sufficiently large.

An actual STSF measurement as outlined above using 1 reference and 13 by 8 hologram grid positions was performed and HIE was applied to

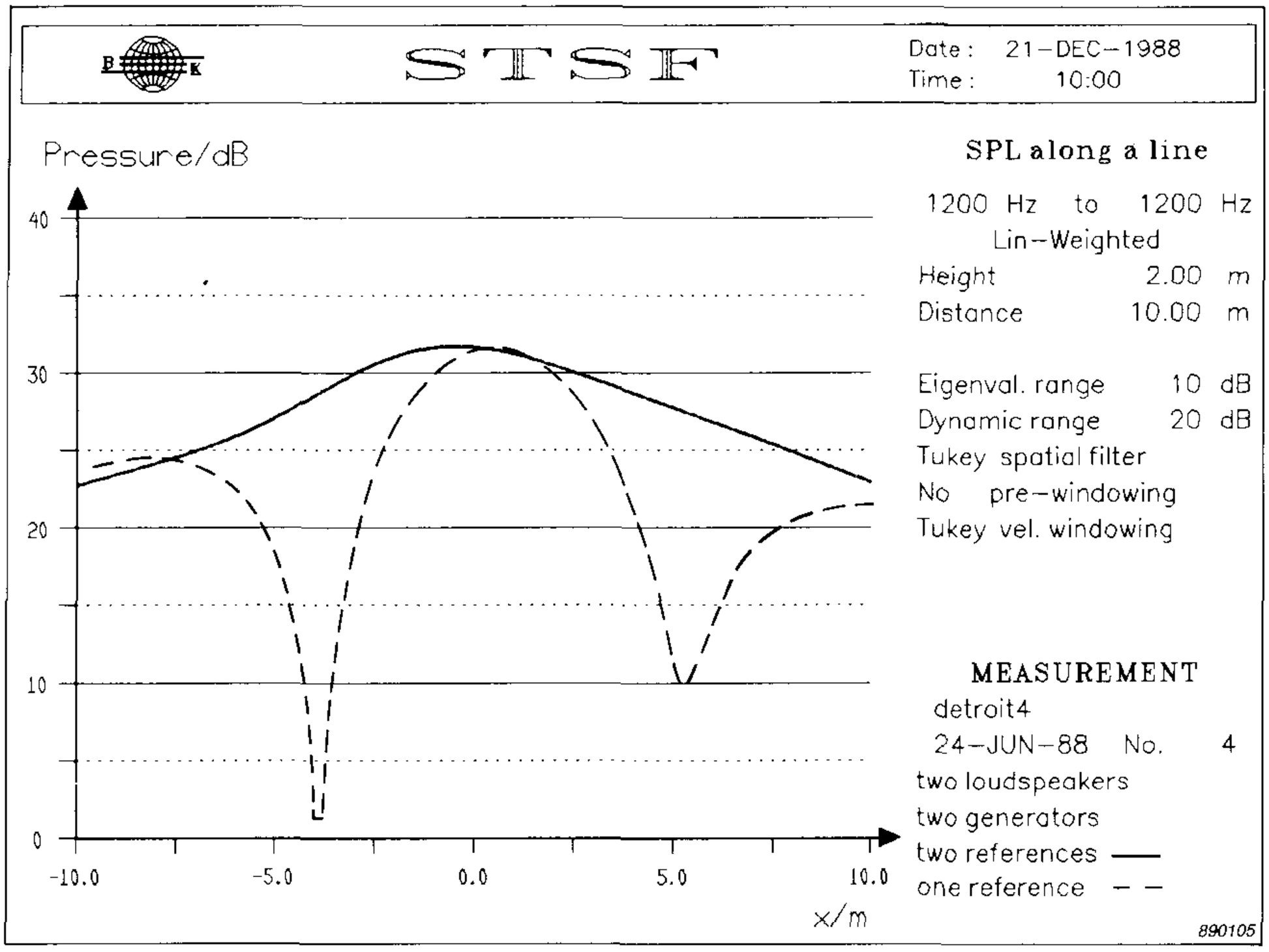

Fig. 6. Calculated sound pressure level along a line for a measurement employing one reference (dashed) and a measurement employing two references (solid)

calculate the sound pressure level along a line in front of the hologram plane. The geometry of the measurement setup was selected as follows:

Hologram grid spacing:	7 cm
Distance from source to hologram plane:	10 cm
Distance between the speakers:	35 cm

and the output line was positioned 10 m in front of the hologram plane. A 100 Hz bandwidth random signal centered at 1200 Hz was applied.

The dashed curve in Fig. 6 shows the calculated sound pressure level. As expected, there is a pronounced interference pattern.

However, since the contributions from the two speakers are actually uncorrelated, the observed interference is entirely due to an incomplete mathematical model of the field. There is no real physical interference.

As discussed previously, the incompleteness of the mathematical model is due to an insufficient set of independent views of the uncorrelated par-

tial fields from the references. At each hologram grid position, only the subspace of views seen from the references is included in the mathematical model (the principal holograms) and subsequently used in calculations. With the arbitrary selection of equal phase of the partial fields at the reference, only the in-phase equal-amplitude view of the two partial fields is included. Most of the hologram grid points, however, have a view including both an in-phase equal-amplitude component and an orthogonal anti-phase equal-amplitude component.

To include both of these orthogonal views in the reference measurement, we need to add another reference. Further, the second reference must have a view of the two partial fields which is different from the view seen by the first reference. For example, the second reference must be positioned away from the symmetry plane, if the position of the first reference in this plane is maintained.

For the present measurement, two different views were obtained by positioning a reference immediately in front of each one of the loudspeakers. By this positioning each reference sees primarily one of the partial fields (loudspeakers), and therefore the views seen by the two references will be almost orthogonal. Complete orthogonality would be achieved, if each reference could see only one partial field. In that case the orthogonal principal views $\boldsymbol{v}_1$ and $\boldsymbol{v}_2$ would be scaled versions of the views seen from the two references. Further, the principal holograms $\boldsymbol{a}_1$ and $\boldsymbol{a}_2$ would equal the partial holograms $\boldsymbol{p}_1$ and $\boldsymbol{p}_2$.

The solid curve in Fig. 6 shows the sound pressure level calculated from the measurement employing two references. Clearly, the spurious interference pattern has been avoided. It should be mentioned that the measurement was taken during a seminar with audience discussions and using a relatively short averaging time.

3.3.5. Strategies for reference selection

The above example leads to a treatment of the following problem: Which general rules can be applied for selection of references, and how can a selected set of references be evaluated.

Theoretically, a set of references provides a sufficient set of views of a composite source, if all the significant views seen from the hologram grid are just included. However, if an important view is present with a very small weight compared with other views, this will show up as an important but relatively small singular value γ_i in the expansion (99) of $\boldsymbol{R}$, and therefore as a relatively small eigenvalue $d_i = \gamma_i^2$ in the eigenvector expansion

(88) of the reference cross spectrum matrix $\boldsymbol{C}_R$. Since this matrix must be inverted in connection with the calculation of the principal holograms (see eqs. (92) and (93)), and since in practice we need to define an eigenvalue threshold in connection with this inversion, the small eigenvalue d_i may be set to zero which will cause the corresponding principal view $\boldsymbol{v}_i$ not to be included. In other words, the set of orthogonal views seen from the hologram grid must be present in the set of reference views with weights of the same order of magnitude.

A criterion for reference selection derived from the above considerations is to select references with the objective of obtaining a maximum number of large eigenvalues d_i of the same order of magnitude.

If no *a priori* knowledge is available about the positions of the independent partial sources, then the straightforward reference selection strategy is to distribute a set of references equally over the source and close to the hologram plane. By doing so, many different views of the source are obtained, and the relative weights of the individual partial fields will be approximately the same over the set of references as over the set of hologram grid positions. Therefore, the eigenvalue threshold in the inversion of $\boldsymbol{C}_R$ will usually exclude only the views which have a relatively small weights over both the references and over the hologram grid.

If one or several partial sources can be identified before the references are selected, then references may be positioned to pick up individual partial fields. In that case, however, special attention must be paid to the requirement that all the important independent views of the set of partial fields must be seen with weights of the same order of magnitude from the set of references.

3.3.6. Validation of a reference selection

Having selected a set of references in connection with a practical measurement, it is important to be able to evaluate, if the selected set of references provides a sufficient set of views of the actual source. For this evaluation we apply the so-called validation procedure which can be explained as follows.

In order to formulate expressions for single cross spectra in the cross spectrum matrices $\boldsymbol{C}$ and $\boldsymbol{C}'$ we define a row matrix $\boldsymbol{w}_n$ constituting row no. n in the matrix $\boldsymbol{P}$ of partial holograms. Thus, $\boldsymbol{w}_n$ contains the view of the L partial fields seen from hologram grid point no. n. Use of this definition in connection with formula (62) for the cross spectrum hologram matrix $\boldsymbol{C}$ allows the element $C_{n\nu}$ in row no. n and column no. ν of $\boldsymbol{C}$ to be expressed in terms of $\boldsymbol{w}_n$ and $\boldsymbol{w}_\nu$:

$$C_{n\nu} = \boldsymbol{w}_n^{\star}\, \boldsymbol{w}_\nu^{T} \tag{112}$$

The element $C_{n\nu}$ is the cross spectrum between hologram grid points no. n and no. ν.

A similar expression can be achieved for the corresponding element $C'_{n\nu}$ in the estimated cross spectrum hologram matrix $\boldsymbol{C}'$. From eqs. (100) and (106) we obtain

$$C'_{n\nu} = (\boldsymbol{w}_n\, \boldsymbol{V}_1^{\star})^{\star} (\boldsymbol{w}_\nu\, \boldsymbol{V}_1^{\star})^{T} \tag{113}$$

This formula expresses the cross spectrum between hologram grid points no. n and no. ν estimated from the measurement of $\boldsymbol{C}_R$ and $\boldsymbol{C}_{\perp}$.

A relation between the true cross spectrum $C_{n\nu}$ and the estimated cross spectrum $C'_{n\nu}$ can be obtained exactly as the corresponding relation between the cross spectrum matrices in eq. (108):

$$C_{n\nu} = C'_{n\nu} + (\boldsymbol{w}_n\, \boldsymbol{V}_2^{\star})^{\star} (\boldsymbol{w}_\nu\, \boldsymbol{V}_2^{\star})^{T} \tag{114}$$

This formula expresses the same as eq. (108), only for single elements of the matrices.

In order to simplify the considerations to follow, we now define a column matrix $\boldsymbol{e}_n$ describing for the view $\boldsymbol{w}_n$ from hologram grid point no. n the content of unit views $\boldsymbol{v}_i$, $i = J+1, J+2, \ldots, L$, not seen from the references:

$$\boldsymbol{e}_n \equiv (\boldsymbol{w}_n\, \boldsymbol{V}_2^{\star})^{T} \tag{115}$$

Use of this definition allows the relation (114) between $C_{n\nu}$ and $C'_{n\nu}$ to be rewritten as follows:

$$C_{n\nu} = C'_{n\nu} + \boldsymbol{e}_n^{\star T}\, \boldsymbol{e}_\nu \tag{116}$$

As a special case ($\nu = n$) we obtain from eq. (116) the following relation between the estimated autospectrum C'_{nn} and the true autospectrum C_{nn} at hologram grid point no. n:

$$C_{nn} = C'_{nn} + \boldsymbol{e}_n^{\star T}\, \boldsymbol{e}_n = C'_{nn} + \left\| \boldsymbol{e}_n \right\|^2 \tag{117}$$

Here, $\| \cdot \|$ represents the length of a complex vector.

From the relation (117) it is evident that the estimated autospectrum C'_{nn} cannot exceed the true autospectrum C_{nn}:

$$C'_{nn} \leqslant C_{nn} \tag{118}$$

If the principal views $\boldsymbol{v}_i$, $i = 1, 2, \ldots, J$, obtained by the set of references, span most of the view $\boldsymbol{w}_n$ seen from the particular hologram grid position,

then $\boldsymbol{w}_n$ has only negligible components along the unit views $\boldsymbol{v}_i$, $i = J+1, J+2, \ldots, L$, not obtained by the references, and thus C'_{nn} will be close to C_{nn}.

An upper bound for the error on the estimate C'_{nv} of the cross spectrum C_{nv} can be derived from eqs. (116) and (117) above. Through application of Schwarz' inequality for a complex unitary vector space we obtain

$$\left| C_{nv} - C'_{nv} \right| = \left| \boldsymbol{e}_n^{\star T} \boldsymbol{e}_v \right|$$

$$\leq \left\| \boldsymbol{e}_n \right\| \left\| \boldsymbol{e}_v \right\| = \sqrt{\left| C_{nn} - C'_{nn} \right| \left| C_{vv} - C'_{vv} \right|} \quad (119)$$

From the inequalities (118) and (119) we conclude as follows. If a given set of references can be shown to provide good estimates C'_{nn} of the auto-spectra C_{nn} over the hologram grid, then we know that good estimates C'_{nv} are obtained for all the cross spectra C_{nv} in the cross spectrum hologram matrix $\boldsymbol{C}$.

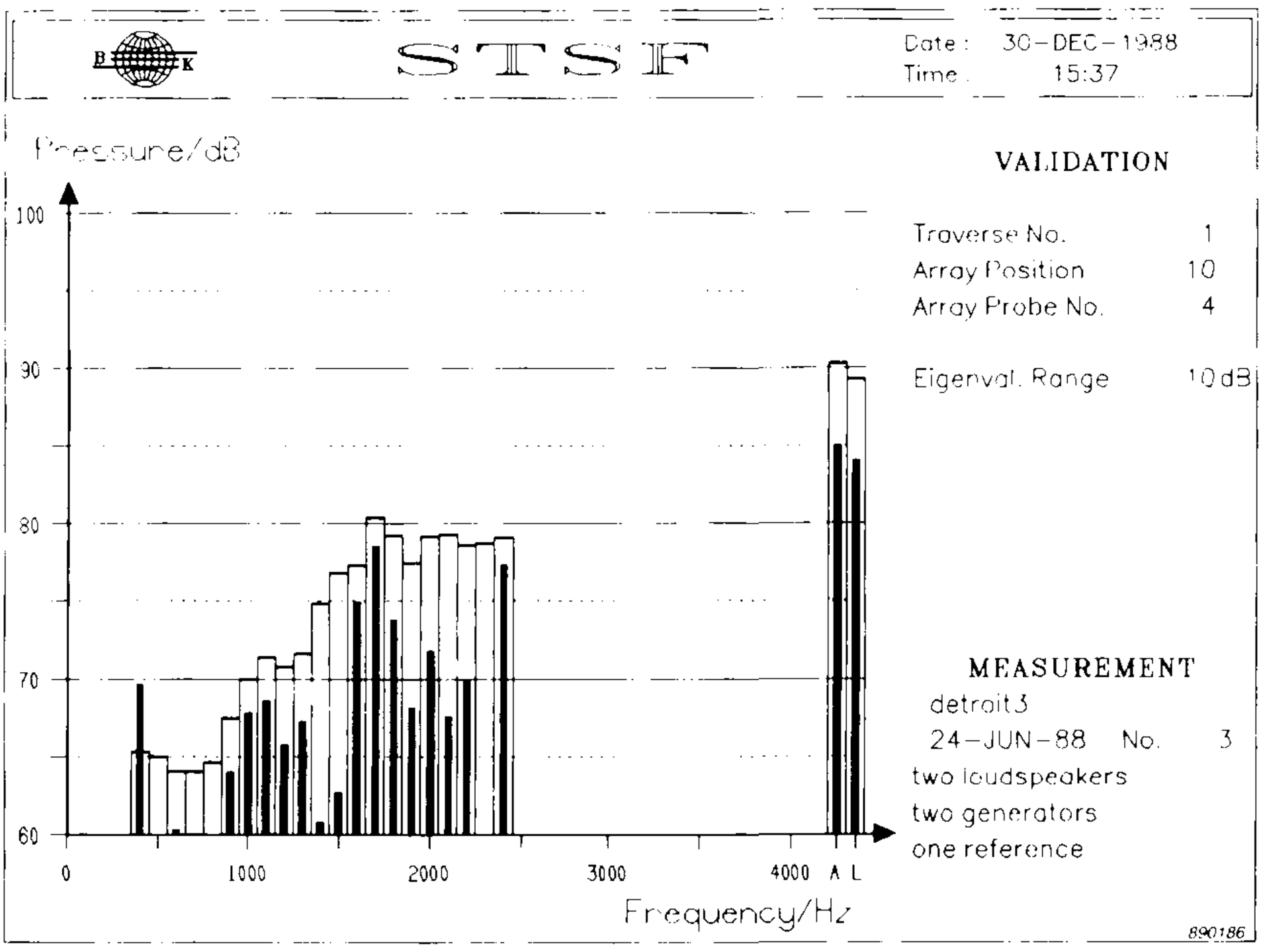

Fig. 7. STSF validation plot for the measurement illustrated in Fig. 5 employing only one reference

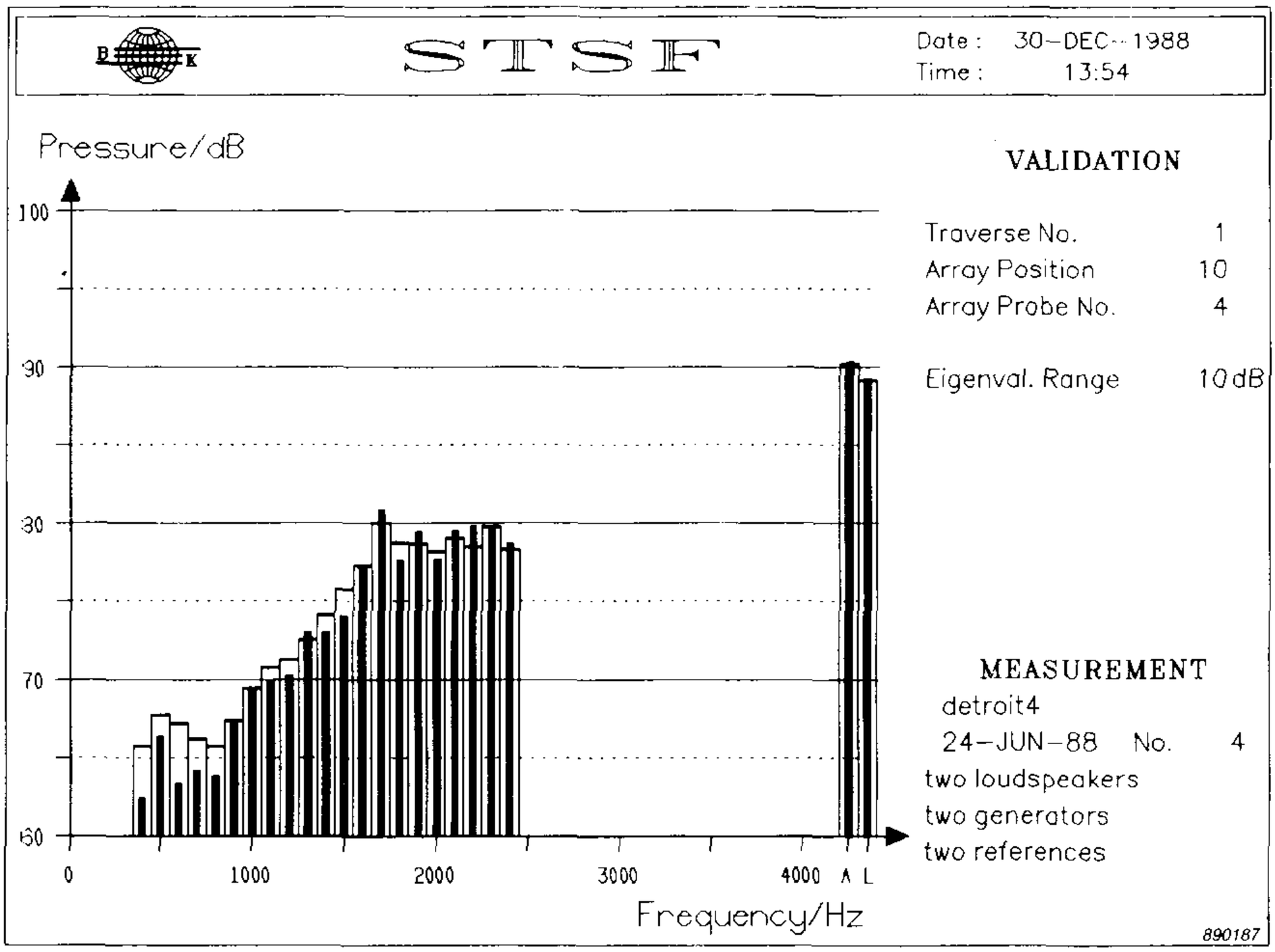

Fig. 8. STSF validation plot for the measurement illustrated in Fig. 5, but with the use of two references

The validation procedure applied in the STSF technique is based on the above conclusion. To enable a comparison of the estimated autospectrum C'_{nn} and the true autospectrum C_{nn}, we measure the autospectrum C_{nn} at each hologram grid position. The estimated autospectrum C'_{nn} is obtained from eqs. (100) and (93). Notice that one hologram grid position can be evaluated separately by measuring only the cross spectra to that particular position from all of the references. These cross spectra constitute one row in $\boldsymbol{C}_{\Delta}{}^{T}$, which in connection with the reference measurement $\boldsymbol{C}_{R}$ allows one row in $\boldsymbol{A}$ and thus one autospectrum on the diagonal of $\boldsymbol{C}'$ to be calculated. The validation procedure can therefore be applied at selected positions over the measurement region before a complete measurement is taken.

Fig. 7 gives an example of application of the validation procedure in connection with the measurement illustrated in Fig. 5 employing only one reference. The two speakers were excited from two broad-band random generators, measurements were performed with a B&K 2032 dual channel

FFT analyzer, and 100 Hz bandwidth spectra were synthesized from the measured narrow-band spectra. Two spectra are shown superimposed for a position in front of the right speaker as seen in Fig. 5: the measured autospectrum C_{nn} (boxes) and the estimated autospectrum C'_{nn} (bars). Clearly, there is a significant deviation between the two spectra.

For comparison Fig. 8 shows the same validation plot for the measurement employing two references. In this case there is good agreement.

3.3.7. Other sources of errors than reference selection

In both Fig. 7 and Fig. 8 there are frequency bands where the estimated autospectrum (sound pressure level) C'_{nn} exceeds the measured autospectrum C_{nn}. This is due to the following types of measurement errors:

- Non-stationarity of the source or the surroundings during the measurement.
- Confidence level of measurements too low due to use of a short averaging time.
- Background noise.

All errors of the types mentioned above have been neglected in the theoretical treatment given previously.

Under the discussion of reference selection, however, the use of an eigenvalue threshold in connection with the inversion of the reference cross spectrum matrix $\boldsymbol{C}_R$ was mentioned. Such a threshold is very important when measurement errors are present.

Considering only the errors in the measurement of the scan cross spectrum matrix $\boldsymbol{C}_\lrcorner$, then provided the errors are random, they will be equally distributed over the unnormalized principal holograms $\boldsymbol{C}_\lrcorner^T \boldsymbol{s}_i$ appearing in eq. (94). In the normalization with $1/\sqrt{d_i}$, these errors will be magnified for principal views $\boldsymbol{v}_i$ and traces $\boldsymbol{s}_i$ which have a small weight (eigenvalue) d_i in the reference measurement. For sufficiently small eigenvalues d_i, the error level will exceed the level of the desired signal. By introduction of a suitable eigenvalue threshold level, it is possible to keep the contribution from these random errors below an acceptable average level over the hologram grid.

Systematic errors, arising in particular from non-stationarity during the measurement, cannot be controlled as efficiently by the eigenvalue threshold. It is therefore very important to ensure a high degree of stationarity during the measurement.

Furthermore, random variations over the hologram grid will/can to a certain extent be removed by spatial filtering in connection with the HIE and NAH calculations on the principal holograms $\boldsymbol{a}_i$. This is not in general possible — at least not as effectively — with systematic errors.

Of outstanding importance is the stationarity during the reference measurement, which constitutes the basis for the entire measurement. No spatial filtering is possible in connection with this measurement. Therefore, a high confidence level should be aimed at by the use of a long averaging time.

The influence of uncorrelated background noise can be more or less eliminated by selection of references which do not pick up the background noise or do it only to a very small extent. Use of a sufficiently long averaging time will then eliminate the background noise from the measurement of the cross spectra, but not from the autospectra measured over the hologram grid for the validation. The validation procedure therefore does not apply in the presence of strong, uncorrelated background noise.

3.3.8. Frequency bandwidth considerations

So far we have considered only monochromatic fields, i.e. fields with only a single frequency component. A general stationary monochromatic field has been modelled as a superposition of a set of mutually uncorrelated time harmonic fields, each of which are perfectly coherent.

In connection with practical measurements on a stationary random broad-band sound source, however, a finite measurement bandwidth must be applied. Use of a broader bandwidth will tend to reduce both the measurement time and the amount of data and data processing.

A few general considerations shall be given concerning the effect of a small frequency bandwidth of the source or equivalently a small frequency bandwidth of the signal analyzer applied for measurement for cross- and autospectra.

In principle, two sources with different frequencies are uncorrelated, when considered over an infinitely long time interval, no matter how small the frequency difference is. Consequently, if we assume a source which has some small bandwidth rather than being monochromatic, then theoretically it consists of an infinite number of uncorrelated partial sources with infinitesimal frequency steps in between. In relation to the sound field model applied in our analysis, the number L of partial sources and partial fields therefore becomes infinitely large. Further, the partial fields will in general have slightly different frequencies.

Considering two partial fields, however, with very small frequency difference, then usually the corresponding partial holograms $\boldsymbol{p}_l$ will have almost the same variation in amplitude and phase over the hologram grid, especially if they are generated by the same basic source mechanism. But partial holograms which are identical apart from a complex scale factor do not contribute independently to the rank I of the cross spectrum hologram matrix $\boldsymbol{C}$. Such partial holograms are seen with the same view from all the hologram grid positions. Consequently they do not cause increased need for independent reference views. Thus, although the number L of uncorrelated partial fields in our sound field model increases towards infinity, the number J of principal holograms representing the cross spectrum hologram matrix $\boldsymbol{C}$ usually remains small.

In the HIE and NAH transformations, however, the bandwidth will introduce some errors, because the simulated propagation of the wave fields is based on the assumption that all the principal holograms are monochromatic with the same frequency. An analysis of these errors is given in references [10] and [11].

3.4. Effect of reference selection on calculated data

The effect of the reference selection on the representation $\boldsymbol{A}$ of the approximate cross spectrum hologram matrix $\boldsymbol{C}'$ has been described in the previous section: only the subspace of views seen from the references are included in $\boldsymbol{A}$ and thus in $\boldsymbol{C}'$.

Consider now the transformed representation $\tilde{\boldsymbol{A}}$. From eqs. (46), (106) and (42) we obtain

$$\tilde{\boldsymbol{A}} = \boldsymbol{H}\boldsymbol{A} = \boldsymbol{H}\boldsymbol{P}\boldsymbol{V}_1^{\star} = \tilde{\boldsymbol{P}}\boldsymbol{V}_1^{\star} \tag{120}$$

which can be split up in expressions for the transformed principal holograms $\tilde{\boldsymbol{a}}_i$ constituting the columns of $\tilde{\boldsymbol{A}}$:

$$\tilde{\boldsymbol{a}}_i = \tilde{\boldsymbol{P}}\boldsymbol{v}_i^{\star} \qquad i = 1, 2, \ldots, J \tag{121}$$

Denoting by $\tilde{\boldsymbol{C}}'$ the cross spectrum output matrix represented by $\tilde{\boldsymbol{A}}$,

$$\tilde{\boldsymbol{C}}' \equiv \tilde{\boldsymbol{A}}^{\star}\tilde{\boldsymbol{A}}^{T} \tag{122}$$

then $\tilde{\boldsymbol{C}}'$ is an approximation to the true cross spectrum output matrix $\tilde{\boldsymbol{C}}$ expressed in eq. (36), and in analogy with formula (108) one easily verifies that

$$\tilde{\boldsymbol{C}} = \tilde{\boldsymbol{P}}^{\star}\tilde{\boldsymbol{P}}^{T}$$
$$= \tilde{\boldsymbol{C}}' + (\tilde{\boldsymbol{P}}\boldsymbol{V}_2^{\star})^{\star}(\tilde{\boldsymbol{P}}\boldsymbol{V}_2^{\star})^{T} \quad (123)$$

Noting that the view of the (calculated) partial fields from an output point constitutes a row in $\tilde{\boldsymbol{P}}$, the above expressions (121) and (123) show the following: At each output point only the part of the view which is seen also from the references contributes to the calculated results.

This statement explains very precisely the results obtained in the example of section 3.3.4, where one reference was applied in connection with two independently excited speakers. On axis the two speakers are seen with approximately the same view as from the reference, and here a good representation of the total field is achieved. In certain directions off axis only an orthogonal view is seen, so here we obtain no representation of the field.

4. Overview of NAH measurement techniques

Chapter 2 gave a short matrix oriented description of the HIE and NAH transform tools, which in their basic forms operate on a complex hologram $\boldsymbol{p}$ for a time harmonic sound field. Chapter 3 described the STSF measurement technique, which allows the NAH and HIE transform tools to be applied in connection with a cross spectral representation of a non-coherent sound field through a set of principal holograms $\boldsymbol{a}_i$. The present chapter gives an overview of different measurement techniques that have been applied to obtain holograms for use in connection with the NAH transform tool. Different types of signal or different measurement conditions may require different measurement techniques.

4.1. Transfer function measurement techniques

This class of techniques is typically based on the use of a controlled external excitation of the sound source. The radiated sound field will then be completely coherent with the excitation signal. In frequency domain notation, the transfer functions p_n/p_o are measured, where p_o is some complex reference signal and p_n is the complex sound pressure at hologram grid position no. n. Apart from an unimportant constant phase factor, the pressure hologram $\boldsymbol{p} = [p_n]$ can then be obtained by multiplying the measured transfer functions with the magnitude $|p_o|$ of the reference signal.

The first presentation [4] of the NAH technique applied a kind of transfer function measurement technique, involving only a single frequency.

Several frequencies can be measured simultaneously by measuring a transfer function spectrum.

Some techniques for measurement of transfer functions do not require a controlled external excitation. Then the basic requirements are perfect coherence of the sound field and the presence of a coherent reference signal. Other techniques, however, require the use of a controlled external excitation.

The advantages of the transfer function method are the possibilities for non-simultaneous measurement such as the use of a scan technique, and for good suppression of interferring uncorrelated background noise. A main disadvantage is the coherence requirement arising from the use of only one reference in connection with non-simultaneous measurements. If no controlled external excitation is applied, then a certain stationarity of the source must be maintained during the measurement procedure.

4.2. Snap shot techniques

As indicated by the name "snap shot", this technique processes a specific time record of the entire sound field obtained by simultaneous recording at all hologram grid positions.

At each hologram grid position $\underline{r}'_n$ the sound pressure $p(\underline{r}'_n, t)$ is recorded over the time interval $0 \leqslant t \leqslant T$. Then, the mathematical propagation of the sound field is done by Fourier transforming the time records $p(\underline{r}'_n, t)$ to a set of spectra $p_n = p(\underline{r}'_n, \omega)$ and subsequently for each frequency ω exposing the hologram $\boldsymbol{p} = [p_n]$ to the NAH or HIE tools. The time domain signal at a given output position is subsequently achieved by inverse Fourier transformation of the calculated spectrum.

The main advantages are independence of coherence and the possibility of animating the calculated time domain signals. For example, the technique applies for time domain studies of the radiation of impulsive noise. Other important advantages are the short measurement time and the fact that source stationarity is not required.

The main disadvantages are the huge amount of transducers and recording equipment necessary to measure simultaneously at each position, the inability to discriminate against uncorrelated background noise and the difficulties in obtaining confident power descriptors of stationary broadband noise fields. Coherence information cannot be obtained from a single measurement.

The requirement for simultaneous recording can be avoided if a reproducible signal is applied in connection with an accurate trigger facility.

The technique has been described and tested by Maynard [17].

4.3. The intensity/pressure technique (BAHIM)

In this method the amplitude and phase of the hologram $\boldsymbol{p}$ are obtained separately in the following way. The amplitude $|p_n|$ at hologram grid position no. n is achieved through measurement of the sound pressure level. The phase Φ is obtained from the sound pressure level and the tangential components (I_x, I_y) of the sound intensity vector $\underline{I}$ by application of the relation

$$\underline{I} = -\frac{|p|^2}{2\rho\omega}\,\underline{\nabla}\Phi \tag{124}$$

To obtain the phase Φ, a two-dimensional spatial integration must be performed, [18].

The technique applies only in connection with perfectly coherent sound fields, which can be explained as follows. The relation (124) is derived for a monochromatic coherent sound field with a well-defined phase. With two mutually uncorrelated monochromatic sound fields, the total intensity is equal to the sum of the contributions from the two fields. Each term in this sum has its own phase function, which cannot in principle be related to the phase function of the other partial field. If the relation (124) is used to calculate a phase for the total sound field, then implicitly a phase has been defined between mutually uncorrelated components. In general this will cause errors if the phase is used in connection with for example HIE or NAH.

A simple example will illustrate this. Assume the intensity/pressure technique applied in connection with the setup in Fig. 5. Thus, the source consists of two small independently excited loudspeakers with a spacing that is large compared with the distance from the speakers to the holograms plane. The hologram obtained by the pressure/intensity technique will exhibit two areas (over the two speakers) with high pressure, and these two areas will have some mutual phase. Therefore, an interference pattern will be predicted in the far-field region by application of HIE.

The effect is similar to that obtained by application of only a single reference in the STSF cross spectral technique, although the explanation is different. In the intensity/pressure technique the entire field in included, but in a wrong way. In the STSF cross spectral technique the total field is not included, but the remainder can be included by adding references. Using only one reference, the STSF technique requires much less measurement and calculation than the intensity/pressure technique.

4.4. The cross spectral technique (STSF)

This is the technique which has been described in detail in the previous chapters. A set of references are selected and the following measurements are taken:

1. The matrix $\boldsymbol{C}_R$ of cross spectra between all pairs of references
2. The matrix $\boldsymbol{C}_\Delta$ of cross spectra from the references to the hologram grid positions.

In case validation is to be used, the autospectra at the hologram grid positions are also needed. With many modern dual channel analyzers (e.g. the B & K 2032/34) the autospectra are obtained simultaneous with the cross spectrum.

From the measured cross spectra $\boldsymbol{C}_R$ and $\boldsymbol{C}_\Delta$ a set of principal holograms $\boldsymbol{a}_i$ are calculated that can be applied in connection with HIE and NAH for calculation of all power descriptors of the sound field. The calculation of the principal holograms requires an eigenvector expansion of $\boldsymbol{C}_R$. However, provided the number of references is much smaller than the number of hologram grid positions, then the calculations involved in establishing this eigenvector expansion and in calculating the principal holograms $\boldsymbol{a}_i$ are negligible compared with the calculations involved in the NAH and HIE calculations.

With only a single reference, the eigenvector expansion becomes trivial. In that case the method is very similar to the transfer function method. Except for conditions where a special transfer function measurement technique is required, the cross spectral technique applying one reference can replace the transfer function technique.

The main disadvantage of the STSF cross spectral technique is the large number of cross spectrum measurements needed in connection with a large complicated broad-band source. In that case, however, no other scan technique applies. The measurement time can be reduced by application of multi-channel measurement systems. As with other scan techniques the source must remain stationary during the measurement procedure.

5. Conclusion

The Spatial Transformation of Sound Fields (STSF) technique consists of the following main components:

- An efficient principal component measurement technique to achieve a cross spectral representation of the sound field.
- A validation procedure to evaluate the representation obtained by a specific set of references.
- NAH and HIE formulated for application in connection with the cross spectral representation of the sound field.

The basic theory has been outlined, and it has been demonstrated that the STSF technique applies to non-coherent broad-band sound sources without the need for simultaneous measurements. The need for several references in the cross spectral technique has been verified and explained. Further, it has been shown that all power descriptors of the sound field can be obtained over a three dimensional region. No other existing technique has the same capabilities.

A paper dealing with STSF instrumentation and applications will follow in a subsequent number of Technical Review.

References

[1] Parrent, G.B.: *"On the propagation of mutual coherence"* J. Opt. Soc. Am. 49, 787 (1959)

[2] Ferris, H.G.: *"Farfield radiation pattern of a noise source from nearfield measurements"* J. Acoust. Soc. Am. 36, 1597 (1964)

[3] Shewell, J.R. & Wolf, E.: *"Inverse diffraction and a new reciprocity theorem"*, J. Opt. Soc. Am. 58, 1596 (1968)

[4] Williams, E.G., Maynard, J.D. & Skudrzyk, E.J.: *"Sound source reconstructions using a microphone array"* J. Acoust. Soc. Am. 68 (1), 340 (1980)

[5] Maynard, J.D., Williams, E.G. & Lee, Y.: *"Nearfield acoustic holography. I: Theory of generalized holography and the development of NAH"* J. Acoust. Soc. Am. 78 (4), 1395 (1985)

[6] Hald, J.: *"Simulation of partial noise source attenuation"*, Noise-Con 85, Proceedings, 453 (1985)

[7] Hald, J. & Ginn, K.B.: *"Vehicle noise investigation using Spatial Transformation of Sound fields"*, ISATA 1987, Proceedings, (1987)

[8] Hald, J. & Ginn, K.B.: "*Spatial Transformation of Sound Fields: principle, instrumentation and applications*", Acoustic Intensity Symposium, Tokyo (1987)

[9] Ginn, K.B. & Hald, J.: "*The effect of bandwidth on Spatial Transformation of Sound Fields measurements*" Internoise '87, Proceedings, 1203 (1987)

[10] Hald, J. "*Development of STSF with emphasis on the influence of bandwidth, Part I: Background and Theory*" Noise-Con'88, Proceedings, 529, 1988)

[11] Ginn, K.B. & Hald, J.: "*Development of STSF with emphasis on the influence of bandwidth*", *Part II: Instrumentation and computer simulation*, Noise-Con 88, Proceedings, 537 (1988).

[12] Goodman, J.W.: "*Introduction to Fourier optics*", McGraw-Hill, New York (1968)

[13] Morse, P.M. & Ingard, K.U.: "*Theoretical Acoustics*", McGraw-Hill, New York (1968)

[14] Veronesi, W.A. & Maynard, J.D.: "*Nearfield acoustic holography (NAH) II. Holographic reconstruction algorithms and computer implementation*", J. Acoust. Soc. Am. **81** (5), 1307 (1987)

[15] Otte, D., Sas, P., Snoeys, R., Ponseele, P.V. & Leuridan, J.: "*Use of principal component analysis and virtual coherences for dominant noise source identification*", Proceedings Second International Seminar on Noise Source Identification and Numerical Methods in Acoustics, Leuven (1987)

[16] Otte, D., Sas, P., Ponseele, P.V.: "*Noise source identification by use of principal component analysis*", Inter-Noise 88, Proceedings, 199 (1988)

[17] Maynard, J.D.: "*Nearfield Acoustic Holography for wideband sources*", Noise-Con 87, Proceedings, 635 (1987)

[18] Loyau, T., Pascal, J., Gaillard, P.: "*Broad-band acoustic holography reconstruction: BAHIM; an experimental method using acoustic intensity*", Inter-Noise 88, Proceedings, 233 (1988)

APPENDIX 1

In relation to eq. (66) we want to prove that $\boldsymbol{C}_1$ and $\boldsymbol{C}_R$ have equal rank. From eqs. (66), (60), (61) and (57) we obtain

$$\boldsymbol{C}_1 = \boldsymbol{Q}^\star \, \boldsymbol{R}^T \tag{A1-1}$$

which shows that

$$\text{rank } (\boldsymbol{C}_1) \leqslant \text{rank } (\boldsymbol{R}) \tag{A1-2}$$

Because of eq. (60) we have

$$\text{rank } (\boldsymbol{R}) = \text{rank } (\boldsymbol{C}_R) \tag{A1-3}$$

and thus from (A1-2) and (A1-3)

$$\text{rank } (\boldsymbol{C}_R) \geqslant \text{rank } (\boldsymbol{C}_1) \tag{A1-4}$$

On the other hand, since $\boldsymbol{C}_R$ is a submatrix of $\boldsymbol{C}_1$ (see eq. (66)) we have

$$\text{rank } (\boldsymbol{C}_R) \leqslant \text{rank } (\boldsymbol{C}_1) \tag{A1-5}$$

Inequalities (A1-4) and (A1-5) now lead to the desired result

$$\text{rank } (\boldsymbol{C}_R) = \text{rank } (\boldsymbol{C}_1) \tag{A1-6}$$

Previously issued numbers of Brüel & Kjær Technical Review

(Continued from cover page 2)

3–1983 Fourier Analysis of Surface Roughness
2–1983 System Analysis and Time Delay Spectrometry (Part II)
1–1983 System Analysis and Time Delay Spectrometry (Part I)
4–1982 Sound Intensity (Part II Instrumentation and Applications)
Flutter Compensation of Tape Recorded Signals for Narrow Band Analysis
3–1982 Sound Intensity (Part I Theory).
2–1982 Thermal Comfort.
1–1982 Human Body Vibration Exposure and its Measurement.

4–1981 Low Frequency Calibration of Acoustical Measurement Systems.
Calibration and Standards. Vibration and Shock Measurements.
3–1981 Cepstrum Analysis.
2–1981 Acoustic Emission Source Location in Theory and in Practice.
1–1981 The Fundamentals of Industrial Balancing Machines and Their Applications.
4–1980 Selection and Use of Microphones for Engine and Aircraft Noise Measurements.
3–1980 Power Based Measurements of Sound Insulation.
Acoustical Measurement of Auditory Tube Opening.
2–1980 Zoom-FFT.
1–1980 Luminance Contrast Measurement.

4–1979 Prepolarized Condenser Microphones for Measurement Purposes.
Impulse Analysis using a Real-Time Digital Filter Analyzer.
3–1979 The Rationale of Dynamic Balancing by Vibration Measurements.
Interfacing Level Recorder Type 2306 to a Digital Computer.
2–1979 Acoustic Emission.
1–1979 The Discrete Fourier Transform and FFT Analyzers.
4–1978 Reverberation Process at Low Frequencies.
3–1978 The Enigma of Sound Power Measurements at Low Frequencies.

Special technical literature

Brüel & Kjær publishes a variety of technical literature which can be obtained from your local Brüel & Kjær representative.
The following literature is presently available:

- ○ Mechanical Vibration and Shock Measurements (English), 2nd edition
- ○ Modal Analysis of Large Structures–Multiple Exciter Systems (English)
- ○ Noise Control (English, French)
- ○ Frequency Analysis (English)
- ○ Catalogues (several languages)
- ○ Product Data Sheets (English, German, French, Russian)

Furthermore, back copies of the Technical Review can be supplied as shown in the list above. Older issues may be obtained provided they are still in stock.

Brüel & Kjær

WORLD HEADQUARTERS: DK-2850 Nærum · Denmark
Telephone: +45 42 80 05 00 · Telex: 37316 bruka dk · Fax: +45 42 80 14 05

Australia (02) 450-2066 · Austria 02235/7550*0 · Belgium 02·242-97 45 · Brazil (011) 246-8149/246-8166
Canada (514) 695-8225 · Finland (90) 80 17 044 · France (1) 64 57 20 10 · Federal Republic of Germany (04106) 4055
Great Britain (01) 954-2366 · Holland 03 402-39 994 · Hong Kong 5-487486 · Italy (02) 52 44 141 · Japan 03-438-0761
Republic of Korea (02) 554-0605 · Norway 02-78 70 96 · Portugal (1) 65 92 56/65 92 80 · Singapore 225 8533
Spain (91) 268 10 00 · Sweden (08) 711 27 30 · Switzerland (042) 65 11 61 · Taiwan (02) 713 9303 · USA (508) 481-7000
Local representatives and service organisations world-wide

ISSN 007–2621
BV 0035–11

Printed in Denmark by Nærum Offset